Structural basis for distinct quality control mechanisms of Drosophila and mammalian GABAB receptor

Shenglan Zhang, Li Xue, Xuehui Liu, Xuejun Cai Zhang, Rui Zhou, Cangsong Shen, Jean-Philippe Pin, Philippe Rondard, Jianfeng Liu

Structural basis for distinct quality control mechanisms of Drosophila and mammalian $GABA_B$ receptor

Shenglan Zhang[1,*], Li Xue[1,*], Xuehui Liu[3,*], Rui Zhou[1], Cangsong Shen[1], Jean-Philippe Pin[5,^], Xuejun Cai Zhang[2,4,^], Philippe Rondard[5,^] , Jianfeng Liu[1,6,^]

[1] Cellular Signaling laboratory, International Research Center for Sensory Biology and Technology of MOST, Key Laboratory of Molecular Biophysics of MOE, School of Life Science and Technology, Huazhong University of Science and Technology, 430074 Wuhan, China;

[2] National Laboratory of Biomacromolecules, CAS Center for Excellence in Biomacromolecules, Institute of Biophysics, Chinese Academy of Sciences,100101 Beijing, China;

[3] Core Facility for Protein Research, Institute of Biophysics, Chinese Academy of Sciences,100101 Beijing,China;

[4] College of Life Sciences, University of Chinese Academy of Sciences, 100049 Beijing, China;

[5] Institut de Génomique Fonctionnelle, Univ. Montpellier, CNRS, INSERM, Montpellier, France;

[6] Guangzhou Regenerative Medicine and Health Guangdong Laboratory, 510005 Guangzhou, China;

*These authors contributed equally to this work.

^ Correspondence to:

Jean-Philippe Pin, Institut de Génomique Fonctionnelle (IGF), Université de Montpellier, CNRS, INSERM, Montpellier, France. Email: jean-philippe.pin@igf.cnrs.fr; Tel: +33 434 35 9289.

or

Xuejun Cai Zhang, Institute of Biophysics, Chinese Academy of Science, 100101 Beijing, China. Email: zhangc@ibp.ac.cn; Tel: +86-10-64889186

or

Philippe Rondard, Institut de Génomique Fonctionnelle (IGF), Université de Montpellier, CNRS, INSERM, Montpellier, France. Email: philippe.rondard@igf.cnrs.fr; Tel: +33 434 35 9278.

or

Jianfeng Liu, Key Laboratory of Molecular Biophysics of MOE, School of Life Science and Technology, Huazhong University of Science and Technology, 430074 Wuhan, China. Email: jfliu@mail.hust.edu.cn; Tel: +86-27-87792031.

Abstract

The main inhibitory neurotransmitter, γ-aminobutyric acid (GABA), acts through both ionotropic $GABA_A$ and metabotropic $GABA_B$ receptors. The $GABA_B$ receptor regulates synaptic transmission at both pre- and post-synaptic levels by activating $G_{i/o}$ proteins. Mammalian $GABA_B$ receptor is a mandatory heterodimer composed of two homologous subunits $GABA_{B1}$ (GB1) and $GABA_{B2}$ (GB2). Its cell surface trafficking is highly controlled by an endoplasmic reticulum retention signal in the C-terminal intracellular region of GB1 that is masked through a coiled coil interaction with GB2. Here, we investigate the cell surface trafficking of the Drosophila *melanogaster* $GABA_B$ receptor, composed of the same homologous subunits dGB1 and dGB2, that plays important functions in fly brain such as circadian rhythm and sleep regulation. In contrast to the mammalian homologs, the endoplasmic retention signal is carried by dGB2, within its second intracellular loop, and not by dGB1. Indeed, dGB1 can reach the cell surface alone and can target dGB2 to the plasma membrane. NMR analysis shows that the coiled coil domain is structurally conserved between flies and mammals. The drosophila coiled coil domain is also essential for the proper functioning of *drosophila* $GABA_B$ receptor quality control. These findings show how a similar quality control system can adapt during evolution for maintaining the subunit composition of a functional heterodimeric receptor.

Introduction

γ-aminobutyric acid (GABA) is the primary inhibitory neurotransmitter in the brain (1). GABA activates both ionotropic $GABA_A$ receptors (2), for fast synaptic inhibition and the metabotropic $GABA_B$ receptor, a G-protein coupled receptor (GPCR), for slow and prolonged synaptic inhibition (3). $GABA_B$ receptor belongs to the class C of the large GPCR family and signals through $G_{i/o}$ proteins. In response to GABA, presynaptic $GABA_B$ receptor inhibits voltage-gated Ca^{2+} channels to block neurotransmitter release, while postsynaptic $GABA_B$ receptor activates G protein-activated inwardly rectifying K^+ channels (GIRKs) to reduce the occurrence of action potentials. $GABA_B$ receptor suppresses the function of adenylyl cyclase and induces $ERK_{1/2}$ and AKT phosphorylation (4-7). Dysfunction of $GABA_B$ receptor has been implicated in neurological and neuropsychiatric disorders, including spasticity, epilepsy, pain, addiction, and anxiety (8, 9).

Mammalian $GABA_B$ receptor are mandatory heterodimers composed of two homologous subunits $GABA_{B1}$ (GB1) and $GABA_{B2}$ (GB2) (10-13) (**Figure 1A**). Each subunit is made of three domains, a large extracellular 'Venus Flytrap' (VFT) domain, a transmembrane (TM) domain, and a cytoplasmic tail. While GB1 is responsible for orthosteric ligand recognition through its VFT domain (14, 15), GB2 couples to G protein through its TM domain (16-18). GB1 possess an R-x-R-type endoplasmic reticulum (ER) retention motif in its cytoplasmic tail (19-21), located close to the C-terminal end of a coiled-coil (cc) domain (21, 22). Formation of this cc domain between GB1 and GB2 masks the GB1 ER retention signal and thus enables cell surface expression of the heterodimer (11, 13, 23, 24).

$GABA_B$ receptor also exists in *Drosophila melanogaster* (25) and is mainly required for modulation of circadian clock circuits (26) and sleep maintenance (27). Three $GABA_B$ receptor subunits (dGB1, dGB2 and dGB3) have been cloned (25). Drosophila GB1 and GB2 subunits (dGB1 and dGB2, respectively) are homologous to the mammalian ones (**Figure 1B-C and Table S1**), and form a functional heterodimer that mediates signal transduction through G_i signaling (25). Surprisingly, the R-x-R-type ER retention motif found in mammalian GB1 subunits is not present in *D. melanogaster*, suggesting a distinct quality control system for cell surface trafficking of the drosophila $GABA_B$ ($dGABA_B$) receptor.

Here, we investigated the cell surface trafficking of dGB1 and dGB2 that remains unknown. We found that dGB1 can reach the cell surface alone, while dGB2 remains in the ER unless it interacts with dGB1. We show that the ER retention involves the intracellular loop 2 (ICL2) of dGB2, and that the intracellular cc domain interaction between dGB1 and dGB2 allows cell surface targeting of the dGB1-dGB2 heterodimer. Structure of the cc domain complex by nuclear magnetic resonance (NMR) demonstrates that this cc domain interaction in the $GABA_B$ is highly conserved between mammals and drosophila. Our data reveal how a similar system can adapt during evolution though maintaining a proper control of the subunit composition of a functional heterodimeric receptor.

Results

dGABA$_B$ receptor cell surface trafficking

While the cell surface trafficking of the two mammalian GABA$_B$ subunits is well understood (11, 13, 21-24), that of dGABA$_B$ receptor remains unclear. We first verified that dGB1 and dGB2 form a functional GABA$_B$ receptor like to the rat subunits (rGB1a and rGB2, respectively) in HEK-293 cells. Indeed, in cells co-transfected with GB1 and GB2 together with a chimeric G protein Gq$_{i9}$ to allow the activation of phospholipase C (28), GABA generated intracellular calcium responses only in cells expressing both GB1 and GB2 subunits, whether from rat or drosophila (**Figure 1D-E**).

We then compared the cell surface expression of dGABA$_B$ receptor and rat GABA$_B$ receptor in HEK-293 cells by ELISA using HA-tagged GB1 and FLAG-tagged GB2 constructs. dGB1 was found to reach the cell surface alone whereas dGB2 failed to do so. Co-expression of dGB1 is sufficient to address dGB2 at the cell surface (**Figure 2A**). We verified using the same assay that rGB1 alone was retained intracellularly, while rGB2 reached the cell surface alone and allowed targeting of rGB1 to the cell surface (**Figure 2B**), as already well demonstrated (19, 20).

We further analyzed the cellular distribution of dGABA$_B$ receptor by confocal immunofluorescence microscopy. dGB2 alone, but not dGB1, co-localized with the ER marker calreticulin (29) (**Figure 2C and Figure S1A**), while dGB1 alone co-localized with the cell membrane marker sodium potassium ATPase (30) (**Figure 2C and Figure S1A**). dGB2 expressed alone did not co-localize with the cell membrane marker (**Figure S1A**). As a control and as expected for the mammalian GABA$_B$ receptor, rGB1 expressed alone was retained in the ER while rGB2 alone was found in the plasma membrane (**Figure 2C and Figure S1A**). These results confirmed that dGB1 can

reach the cell surface alone while dGB2 is retained in the ER, but these two subunits are co-localized at the plasma membrane when co-expressed together, similarly to the rat subunits (**Figure 2D and Figure S1B**).

Finally, we show that co-transfected HA-dGB1 and FLAG-dGB2 also co-localized in drosophila S2 cells (**Figure S1C**). In contrast to dGB1, dGB2 alone failed to reach the drosophila S2 cell surface and dGB1 facilitated its cell surface expression of dGB2, as shown in ELISA experiments (**Figure S1D**). Altogether, these data demonstrate that cell surface trafficking of $dGABA_B$ receptor subunits is controlled by ER retention of dGB2, while dGB1 is responsible for cell surface targeting of the functional $GABA_B$ heterodimer.

To investigate the molecular determinants responsible for the dGB2 ER retention in HEK-293 cells, we generated different dGB2 constructs by replacing different regions of dGB2 by that of rGB2, such as the C-terminal region including the cc sequence ($dGB2^{rGB2C}$; **Figure S1E**) or the different ICL region ($dGB2^{rICL1}$, $dGB2^{rICL2}$ and $dGB2^{rICL3}$) (**Figure 2E**). Only $dGB2^{rICL2}$ expressed alone reached the cell surface, whereas $dGB2^{rICL1}$ and $dGB2^{rICL3}$ were still retained inside the cell. $dGB2^{rGB2C}$ expressed alone co-localized with calreticulin in ER (**Figure S1E**), indicating that the ER retention signal of dGB2 is not located within its C-terminal intracellular region. Altogether, our data revealed that the ICL2 region is an important determinant for the intracellular retention of dGB2.

Coiled-coil domain is critical for cell surface trafficking of $dGABA_B$ receptor

The cc interaction in the C-terminal region of mammalian GB1 and GB2 is required for $GABA_B$ cell surface targeting (21, 22). A cc region at a similar position in both dGB1 and dGB2 can be predicted

using the freely available COILS program (31) (**Figure S2A-B**). To investigate the importance of this region for dGABA$_B$ subunits trafficking, we generated dGB1 and dGB2 mutants with truncature immediately after (ΔC1) or before (ΔC2) these predicted cc regions, and named these constructs dGB1$^{\Delta C1}$, dGB2$^{\Delta C1}$, dGB1$^{\Delta C2}$ and dGB2$^{\Delta C2}$ (**Figure 3A-C**). dGB1 facilitated cell surface expression of dGB2$^{\Delta C1}$ and wild-type dGB2 that could form a cc interaction, but not of dGB2$^{\Delta C2}$ that could not do it (**Figure 3B and Figure S3D**). Similarly, wild-type dGB1 and dGB1$^{\Delta C1}$ facilitated cell surface expression of wild-type dGB2, but not of dGB1$^{\Delta C2}$, and it was not due to a loss of cell surface trafficking of dGB1$^{\Delta C2}$ (**Figure 3C and Figure S3D**). The data showed that the predicted cc domain of dGB1 and dGB2 are necessary for dGABA$_B$ receptor cell surface trafficking.

Similar conclusions can be reached by analyzing the cellular distribution of these mutants by confocal immunofluorescence microscopy. The ΔC1 construct of one subunit can traffick to the cell surface when co-expressed with the other wild-type subunit (**Figure 3D and Figure S3C**), to form a functional heterodimer as shown by intracellular calcium release (**Figure 3E**). In contrast, the GB2$^{\Delta C2}$ construct cannot traffick to the cell surface when co-expressed with the wild-type GB1 subunit (**Figure 3D and Figure S3C**), in agreement of the functional response mediated by these constructs (**Figure 3E**). Of note, dGB2$^{\Delta C1}$ and dGB2$^{\Delta C2}$ expressed alone remains localized in ER (**Figure S3A**), while dGB1$^{\Delta C1}$ and dGB1$^{\Delta C2}$ alone reached the cell surface (**Figure S3B**).

dGABA$_B$ coiled-coil interaction is highly specific

The cc region in both dGABA$_B$ subunits shows a high similarity of sequences with that of human and rat receptors (**Figure S2B**). We examined whether the wild-type dGB1 and dGB2 could traffick and

form a functional receptor when co-expressed with the complementary rat subunits. Interestingly, dGB1 and rGB2, two subunits that can traffick to the cell surface alone, formed a functional receptor at the cell surface (**Figure 4A-C**). In contrast, the rGB1 and dGB2 that are individually retained in the ER were not able to traffick to the cell surface when co-expressed and then did not form a functional receptor (**Figure 4D-F**). But when using chimeric rGB1 ($rGB1^{dGB1C}$) and dGB2 ($dGB2^{rGB2C}$) generated by replacing the C-terminal of rGB1 and dGB2 by those of dGB1 and rGB2 respectively, a functional receptor could be obtained when these constructs were co-expressed with specific subunits (**Figure 4D-G and Figure S4A-C**). Indeed, the $rGB1^{dGB1C}$ chimera could form a functional receptor with dGB2 more efficiently compared to the subunit rGB1 co-expressed with $dGB2^{rGB2C}$ (**Figure 4E-F)**. Altogether, these results showed that cc domain interaction is crucial to release ER retention and to allow cell surface targeting of the heterodimer.

Structural basis of $dGABA_B$ coiled-coil domain

We have solved the three-dimensional structure of the heterodimeric dGB1:dGB2 cc domain by NMR. Since the R-x-R ER retention motif ($_{923}$RSRR$_{926}$) in mammalian $GABA_B$ (22) was not involved in this cc interaction, we used a polypeptide from dGB1 that does not contain this retention motif (dGB1cc; residues 755–796) and another one from dGB2 with an equivalent sequence (dGB2cc; residues 741–780). To obtain the complex dGB1:dGB2, we have co-expressed the untagged dGB1cc with the glutathione-S-transferase-tagged dGB2cc. The ^{13}C-^{15}N isotope-labeled dGB1cc:dGB2cc complex was purified for NMR experiments (**Figure S5A**). In order to avoid aggregation, two cysteines of dGB2 (residue 743 and 757) were replaced by a serine residue. The ^{1}H-^{15}N hetero-nuclear single quantum

coherence (HSQC) spectrum is well dispersed (**Figure S5B**) and solution structures of the heterodimeric cc complex were calculated and modeled. Structural statistics of the ensemble of 20 lowest energy conformers that represent the solution structure was summarized (**Table S2**), and a backbone superimposition of these conformers was produced (**Figure 5A**). Residues 755–794 and 741–778 of dGB1 and dGB2 respectively, are well-defined α-helices with a Cα ensemble root mean square deviation (RMSD) of 0.63 ± 0.22 Å (**Table S2**), while a few residues flanking the cc region were flexible.

The overall structure of the complex consists of a left-handed and two-stranded parallel cc interaction **(Figure 5A-B)**. Residues encoding canonical cc domains are characterized by heptad periodicity repeats, denoted $[abcdefg]_n$, and the hydrophobic core exhibits a classical "knobs-into-hole" packing proposed by Crick (32), in which hydrophobic side chains at *a* and *d* position from one helix act as "knobs" and insert into "holes" formed by four residues on the other helix. The dGB1cc:dGB2cc complex contains five completed canonical heptad repeats, denoted $[abcdefg]_n$ for dGB1 and $[a'b'c'd'e'f'g']_n$ for dGB2, and additional cc residues at both N- and C- termini (**Figure 5B-C**). The helices interact through a series of side chains in the cc interface to form the classic "knobs" (**Figure 5D**). Most of the highly conserved hydrophobic residues, in particular leucines and isoleucines (in dGB1cc, L765, L772, I776, I783, L786 and L790; in dGB2cc, L745, L749, L763, L770, L773 and L777), dominantly occupy these *a* and *d* positions and form the hydrophobic core of the heterodimeric cc structure (**Figure 5B and 5D**).

Except this canonical hydrophobic packing, additional short-distance hydrogen bonds and charge-charge interactions probably contribute to the stabilization of the cc interaction. Specially, a pair of highly conserved asparagines at a_3/a_3' positions of the two α-helices ("knob"), $dGB1^{N769}$ / $dGB2^{N756}$,

stay close (distance of Cγ, 4.71 ± 0.46 Å), forming a probably hydrogen bond through their side chains (**Figure 5E and Figure S2B**). Moreover, two pairs of charged residues which occupy d_4/d_4' and e_4/e_4' positions, K779 / K766 and E780 / E767 respectively, are also close enough to form inter-helical salt bridges (distances between Cε of K779 and Cδ of K766, and between Cδ of E780 and Cε of E767 are 5.48 ± 1.15 Å and 3.83 ± 0.25 Å, respectively) (**Figure 5E**). These two adjacent salt bridges may contribute strongly to stabilize the cc complex.

To investigate the importance of these residues in stabilizing the cc interaction, we have replaced these residues in dGB1 and dGB2 at *a/a'*, *d/d'* and *e/e'* positions (a_1/a_1', a_2/a_2', a_3/a_3', a_4/a_4', a_5/a_5', a_6/a_6'; d_1/d_1', d_2/d_2' d_3/d_3', d_4/d_4', d_5/d_5' and e_4/e_4') to change their polarity (**Figure 5F**). We have co-transfected each individual mutant with the other wild-type subunit. Several of these dGB1 mutants such as L772D (d_3), I783D (a_5) and L786D (d_5) failed to bring dGB2 to the cell surface (**Figure 5F**). Similarly, wild-type dGB1 failed to carry some dGB2 mutants such as E767K (e'_4), L770D (a'_5) and L773D (d'_5) to cell surface (**Figure 5G**). Together, these data further confirmed that cc interaction is responsible for cell surface trafficking of $dGABA_B$ receptor.

To compare these structural models in solution with previous crystal structures of the $GABA_B$ mammalian cc domain (22), the overall structural backbones were superimposed based on the sequence alignment of the constructs (**Figure S6A-B**). Although there are less polar residues in drosophila cc interaction, the main mechanism to stabilize the cc interaction is mainly hydrophobic interactions as reported in mammalian $GABA_B$ receptor. The central cc region is highly conserved between mammalians and drosophila (**Figure S6C**), with a conserved hydrogen-bonded interaction between two Asn residues between dGB1 and dGB2 (**Figure S6D**). But among two adjacent salt bridges identified in the NMR structure, only one was conserved in mammalian cc domain (**Figure**

S6E).

Among the conserved hydrophobic residues in the middle of the dGB2 cc region **(Figure S2B)**, Val752 and Phe759 have been changed for their equivalent residue (Leu) in mammalian GB2. Interestingly, the mutants dGB2^{V752L} and dGB2^{F759L} restored the capacity of dGB2 to mask the retention signal on rGB1 (**Figure 6A**), to form a functional receptor (**Figure 6B**) at the cell surface (**Figure 6C and Figure S4D-E**). As a control, with recombinant proteins, we showed that the glutathione S-transferase fused to the dGB2cc was able to pull-down the purified His-tagged cc region of rGB1, confirming the cc interaction between the two subunits (**Figure S7**). These data showed that a single mutation in the cc domain was able to restore the cc interaction between rGB1 and dGB2 and a correct trafficking of a functional $GABA_B$ receptor.

Discussion

The heterodimeric $GABA_B$ receptor has already been characterized in several insects, including drosophila (25), cockroach (33) and the tobacco budworm (34). Like in mammals, this receptor is composed of two subunits, GB1 and GB2. While the mechanism involved in the specific targeting of mammalian heterodimers to the cell surface - a mechanism that guarantees trafficking of functional receptors only - is well characterized, this mechanism is unknown in insects. Sequence analysis revealed that the retention signal found in mammalian GB1 is not found in the insect sequences **(Figure S8A)**. In the present study, we have identified key determinants for cell surface trafficking of the drosophila $dGABA_B$ receptor. First, we have demonstrated that, in contrast to the mammalian subunits, the GB2 subunit contains an intracellular retention signal, while insect GB1 that can reach the cell surface alone. Our biochemical and structural data demonstrate that even though the retention signal is located at a different place, and in the other subunit, the structural element involved in the control of cell surface targeting of the properly assembled heterodimer is conserved during evolution. Indeed, in both mammals and insects, a conserved cc interaction between the proximal C-terminal region of the two subunits dGB1 and dGB2 is necessary to release the subunit retained in the ER.

Evolutionary analysis of the GB1 C-terminal sequences revealed that both di-leucine internalization ($_{886}$EKSRLL$_{891}$) and the ER retention ($_{923}$RSRR$_{926}$) signals of mammalian GB1 appeared during animal evolution **(Figure S8A)**. The RSRR motif is highly conserved in chordates (such as mammals, birds, reptiles, amphibians and fishes) but not in other animals, while the di-leucine motif is not strictly conserved in chordates. This clearly raises the question on how can the correct assembly of functional $GABA_B$ receptors be controlled in non-chordate animals. Our data revealed that in drosophila, this is the dGB2 subunit that is retained in the ER, and trafficked to the cell surface

after its proper interaction with dGB1. Our data show that the sequence element responsible for dGB2 retention in the ER is not located within its large intracellular C-terminal domain. Not only it does not contain an RSRR motif, like the one found in chordate GB1s, but mutation of any possible ER retention motifs located before ($_{724}$RVR$_{726}$), inside ($_{748}$RLR$_{750}$, $_{758}$RFR$_{760}$ and $_{724}$RVR$_{726}$), or after ($_{860}$KKKK$_{863}$, $_{956}$RERR$_{959}$ and $_{1189}$LL$_{1190}$) the cc region failed to release dGB2 from ER (data no shown). The surface trafficking of rat-drosophila GB2 chimera revealed that the GB2 ICL2 is involved in its ER retention. This is surprising considering the high conservation of this loop between dGB2 and rGB2 (75% and 62.5% in similarity and identity, respectively) (**Figure S8B**). However, intracellular retention signals have already been identified in the intracellular loops of other GPCRs, such as ICL1 (35) (36) or ICL2 loops (37). Although it is possible that an ER retention motif could be found within the few positions that differ between rat and drosophila GB2 ICL2, we cannot also exclude the possibility that the presence of the rat ICL2 within dGB2 mask a retention signal located elsewhere in the dGB2 sequence. Clearly, more work is needed to clarify this point.

Several partner proteins are involved in the control of the cell surface targeting of correctly assembled mammalian $GABA_B$ receptors. First, COPI (coat protein complex I) specifically binds to the GB1 ER retention signal, releasing any GB1 proteins that escape from the ER to reach the *cis*-golgi to redirect it to the ER in COPI-coated vesicles (38). Second, Msec7-1 (Cytohesin), a guanine-nucleotide-exchange factor for the ARF family of GTPase, interacts with GB1 via the di-leucine signal sequence, increasing GB1 cell-surface expression, leading to the COPI-regulated $GABA_B$ receptor trafficking (39). More recently, PRAF2, an ER-resident transmembrane protein, acts as a gatekeeper via its interaction with GB1 through the ER retention signal and the di-leucine signal sequence, retaining GB1 in the ER (40). Of note, homologs of all these proteins can be found in the Drosophila

genome (41-43), but their possible role in the dGB2 retention remains to be established.

Our study reveals a high conservation of the cc domain structure during evolution of the $GABA_B$ receptor, from flies to human. This suggests an important role for this domain involved in both the correct assembly of the $GABA_B$ heterodimer, and the correct trafficking to the cell surface of the functional receptor. Although well-conserved, we show that some divergence on the determinants essential for the proper interaction between the subunits exist. The interaction dGB1cc:dGB2cc is more hydrophobic than the mammal ones mainly stabilized by a larger number of polar interactions and salt bridges (22) **(Figure 6E)**. Whatever, leucine residues seem important molecular determinants for a stable cc domain interaction, as indicated by the introduction of a single Leu in dGB2, either at position 752 and 759 and conserved in chordates, that is sufficient to restore the interaction with the rGB1 cc domain. It shows the high selectivity of interactions between the cc domains within the heterodimer.

In conclusion, it is fascinating to see how the ER retention system is involved to control the correctly assembled $GABA_B$ receptors. Although based on the ER retention of one subunit, either GB1 in chordates, or GB2 in insects, the same cc domain resulting from the correct assembly of the $GABA_B$ subunits and necessary for a functional receptor, is involved in the control of the cell surface trafficking of the receptor. This is of interest when considering that different modes of ER retention are involved. Since the RSRR motif is not conserved in the insect $GABA_B$ receptors, it could be speculated that their GB1 is targeted to the cell surface even in the absence of GB2 subunit, while GB2 alone might be intracellularly retained. This is opposite to what is occurring in mammals in which the GB2 subunits can reach the cell surface alone, but, being unstable in the absence of GB1, is rapidly degraded, as shown by the low expression of GB2 in GB1-KO mice (44, 45). Such a quality control system is well optimized in mammals where the GB2 subunit expression appears as the driving force for the

expression of a functional $GABA_B$ receptor, as the GB1 subunit is expressed at higher levels, and in a larger number of cells. Whether the opposite is true in insects remains to be established, but this would be consistent with our present data.

Methods and materials

Materials

GABA (γ-aminobutyric acid) and copper sulfate were purchased from Sigma-Aldrich (St. Louis, MO, USA). Lipofectamine 2000 and Fluo4-AM were obtained from Life Technologies (Carlsbad, CA, USA).

Plasmids and transfection

The pRK5 plasmids encodes HA-tagged wild-type rat GB1a and Flag-tagged wild-type rat GB2 were previously described (46). Drosophila GB1 residue 29 – 840 and drosophila GB2 residue 24 – 1220 were seperately constructed in pRK vector plasmid following a plasma membrane signal peptide of metabotropic glutamate receptor 5 (mGluR5) as wild-type dGB1 and dGB2. HA or Flag epitope was inserted just after this signal peptide. The pMTV5-His-A plasmids contained the same open reading frame as drosophila pRK5 plasmids. The pMTV5-His-A plasmids contained the same open reading frame as drosophila pRK5 plasmids. Leucine substitutions and stop mutants were generated by site-directed mutagenesis using the QuikChange mutagenesis protocol (Agilent Technologies).

HEK-293 cells (ATCC, CRL-1537) were cultured in Dulbecco's modified Eagle's medium (DMEM) supplemented with 10% fetal bovine serum at 37°C under 5 % CO_2. Cells were transfected with pRK5 plasmids using Lipofectamine 2000. Two millions cells were transfected with 0.5 µg of each plasmid of interest. For determination of intracellular calcium measurements, the cells were also transfected with the chimeric G-protein Gqi_9, which allows the coupling of the recombinant $GABA_B$ receptor to the phospholipase C (28).

Drosophila S2 cells (ATCC, 1963) were cultured in ESF 921 insect cell culture medium supplemented with 10% fetal bovine serum at 27°C. Cells were transfected with pMTV5-His-A plasmids using Lipofectamine 2000. Six million cells were transfected with 1 µg of each plasmid of interest. Additional 0.5 mM copper sulfate was added to induce recombinant expression of $GABA_B$ receptor.

Cell surface quantification by ELISA

Detection of the HA- and Flag-tagged constructs at the cell surface by ELISA was performed, as previously described (47). Twenty-four hours after transfection, HEK-293 or *drosophila* S2 cells were seeded into 96-well microplates. Cells were fixed with 4% paraformaldehyde, blocked with 10% FBS. HA-tagged constructs were detected with a monoclonal rat anti-HA antibody coupled to horseradish peroxidase (Roche). Flag-tagged constructs were detected with a monoclonal mouse anti-FLAG antibody coupled to horseradish peroxidase (Sigma-Aldrich). Bound antibodies were detected by chemoluminescence using SuperSignal substrate (Pierce) and a 2103 EnVision™ Multilabel Plate Reader (Perkin Elmer, Waltham, MA, USA).

Immunocytochemistry

Twenty-four hours after transfection, HEK-293 cells or *drosophila* S2 cells were plated on glass coverslips or 35-mm glass bottom culture dishes coated with 0.1 mg/mL poly-D-lysine and incubated. Cells were fixed with 4% paraformaldehyde, permeabilized with 0.1 % Triton-X100 or cold methanol if necessary, blocked with 10% fetal bovine serum, incubated with primary antibody and labeled with secondary antibody. Primary antibodies included rabbit monoclonal anti-HA (1:400, Cell Signaling Technology), mouse monoclonal anti-HA (1:400, Cell Signaling Technology), mouse monoclonal anti-

Flag (1:800, Cell Signaling Technology), rabbit monoclonal anti-Flag (1:800, Cell Signaling Technology), rabbit polyclonal anti-calreticulin (1:200, Abclonal) and rabbit monoclonal anti-Na,K-ATPase α1 (1:100, Cell Signaling Technology). Secondary antibodies included goat anti-mouse and goat anti-rabbit Alexa Fluor 488 (both 1:300, Abclonal), goat anti-mouse and anti-rabbit Alexa Fluor 647 (both 1:300, Abclonal).

Confocal microscopy and data analysis

Imaging of immunostained samples were done by using a confocal laser scanning microscope FV3000 (Olympus, Tokyo, Japan) in College of Life Science and Technology, Huazhong University of Science and Technology. Images were processed and fluorescence (yellow in merge panels) was quantified with Image J plugin JACOP using Manders' co-localization coefficients M1&M2. .

Intracellular calcium release measurements

Twenty-four hours after transfection, HEK-293 cells were seeded into 96-well microplates. Cells were washed by HBSS buffer (20 mM HEPES pH 7.4, 1 mM $MgSO_4$, 3.3 mM Na_2CO_3, 1.3 mM $CaCl_2$, 0.1% BSA and 2.5 mM probenecid) and loaded with 1 μM Ca^{2+}-sensitive fluorescent dye Fluo-4 AM (Molecular Probes, Eugene, OR, USA) for 1h at 37 °C. Cells were then incubated with buffer and added 2×GABA solution at various concentrations after 20 s of recording. Fluorescence signals (excitation at 485 nm, emission at 525 nm) were measured for 60 s by the fluorescence microplate reader Flexstation (Molecular Devices, Sunnyvale, CA, USA). Data were analyzed with Soft Max Pro (Molecular Devices, Sunnyvale, CA, USA). Dose-response curves were fitted using Prism (GraphPad software, San Diego, CA, USA).

Recombinant expression and purification of coiled-coil

The plasmid encoding for rGB1cc, rat GB1a amino acids 909 – 948 was inserted into the Pet-28a (+) vector with a N terminus 6*His–tag. The plasmid dGB2cc, the gene encoding *drosophila* GB2 amino acids 741–780 was inserted into the pGEX-6p-1 vector with a N terminus GST–tag followed by a PreScission cleavage site. The vector pGEX-6p-1 was introduced as the GST negative control. For heterodimeric dGB1cc/dGB2cc, untagged *drosophila* GB1 encoding amino acids 755– 796 and GST–tagged *drosophila* GB2 encoding amino acids 741–780 with serine substitutions (C743S and C757S) were co-expressed.

All the constructs were expressed using *E.coli* strain BL21 (DE3). Specially, uniformly isotope-labeled dGB1cc/dGB2cc was prepared by growing bacterias in M9 minimal medium using $^{15}NH_4Cl$ (Cambridge Isotope Laboratories Inc.) as the sole nitrogen source and $^{13}C6$-glucose (Cambridge Isotope Laboratories Inc.) as the sole carbon sources.

Recombinant expression was induced at 37°C for 3 hours with additional 1 mM IPTG. Bacterials were harvested and lysed. His-tagged rGB1cc was purified by Ni-NTA Agarose affinity chromatography (QIAGEN) followed by Superdex-75 size exclusion chromatography (GE Healthcare). GST, GST-tagged wild-type and mutants of dGB2cc were purified using Glutathione Sepharose High Performance affinity chromatography (GE Healthcare) followed by Superdex-75 size exclusion chromatography. Isotope-labeled dGB1cc/dGB2cc heterodimer were purified using Glutathione Sepharose High Performance affinity chromatography (GE Healthcare), diggested by PreScission protease to remove GST fusion protein followed by Superdex-75 size exclusion chromatography (GE Healthcare).

NMR Spectroscopy and structure calculation

The protein concentration of the isotope-labeled dGB1cc/dGB2cc with C743S and C757S

substitutions was 1.0 mM, dissolved in 20 mM pH 7.0 phosphate buffer (100 mM NaCl, 1 mM TCEP and 0.02% NaN_3). All NMR spectra were acquired at 293 K on an Agilent DD2 600 spectrometer equipped with a cold probe. The sequential backbone resonance assignments were achieved by using standard triple-resonance experiments: HNCACB, CBCA(CO)NH and HNCO (48, 49). Non-exchangeable side chain resonance assignments were carried out with the help of the following spectra: HBHA(CO)NH, C(CO)NH and 13C-edited NOESY (49, 50). Inter-proton distance restraints were derived from 3D NOESY spectra (all with 100 ms mixing time): ^{13}C-edited NOESY and ^{15}N-edited NOESY. The spectra were processed with the program of NMRPipe (51) and analyzed with CcpNmr (52). Structures calculation and NOE assignment were performed simultaneously by using the program CNS (53, 54) and ARIA2 (55). Hydrogen bonding restraints were generated from the standard secondary structure of the protein based on the NOE patterns and backbone secondary chemical shifts. Backbone dihedral angle restraints (ϕ and ψ angles) were derived using the program DANGLE (56) incorporated in the CcpNmr software package. A total of 200 structures were calculated and the 20 structures with the lowest total energy and least experimental violations were selected to perform a refinement procedure in water. The refined structure ensemble was selected to represent the dGB1cc/dGB2cc structure. The atomic coordinate have been deposited in the Protein Data Bank with the accession code of 5X9X and the chemical shift assignments of the domain have been deposited in the Biological Magnetic Resonance Data Bank with accession number of 36064. The protein structure ensemble was displayed and analyzed with PyMol (Palo Alto, CA, USA).

GST pull-down assay

2 μg bacterial purified GST control or GST-fusion protein were immobilized on Glutathione Sepharose High Performance beads (GE Healthcare). After incubation with 2 μg purified His-tagged protein,

beads were recovered and washed with PBS. Protein bound to the beads was eluted with SDS sample buffer and analyzed by SDS-PAGE with Coomassive blue staining.

The molecular model of mammalian $GABA_B$ receptor VFT (PDB code 4MS3 (15)) and coiled-coil domain (PDB code 4PAS) were generated with PyMol.

Statistical analysis

Data are presented as means ± SEM of at least three independent experiments. Statistical analyses were analyzed by GraphPad Prism using one-way ANOVA test followed by a Dunnett's multiple comparisions test. Values with $P < 0.05$ were considered statistically significant.

Acknowledgments

J. L. was supported by the Ministry of Science and Technology (grant number 2018YFA0507003), the National Natural Science Foundation of China (NSFC) (grant numbers 81720108031, 81872945, 31721002 and 31420103909), the Program for Introducing Talents of Discipline to the Universities of the Ministry of Education (grant number B08029), and the Mérieux Research Grants Program of the Institut Mérieux. P. R. and J.-P. P. were supported by the Centre National de la Recherche Scientifique (CNRS) and the Institut National de la Santé et de la Recherche Médicale (INSERM).

Author contributions

S.Z., L.X. and C.S. performed molecular biology and ELISA assays; L.X. and R.Z. performed intracellular calcium assays; S.Z. performed recombinant protein purification and

immunocytochemistry experiments; S.Z. and X.L. performed NMR experiments and structure calculations; S.Z., X.Z., P.R., J.P. and J.L. wrote the manuscript with input from all authors.

Competing financial interests statement

The authors declare no competing financial interests.

References

1. Sivilotti, L., and Nistri, A. (1991) GABA receptor mechanisms in the central nervous system. *Progress in Neurobiology* **36**, 35-92
2. R L Macdonald, a., and Olsen, R. W. (1994) GABAA Receptor Channels. *Annual Review of Neuroscience* **17**, 569-602
3. Curtis, D. R., and Lacey, G. (1998) Prolonged GABAB receptor-mediated synaptic inhibition in the cat spinal cord: an in vivo study. *Experimental Brain Research* **121**, 319-333
4. Baloucoune, G. A., Chun, L., Zhang, W., Xu, C., Huang, S., Sun, Q., Wang, Y., Tu, H., and Liu, J. (2012) GABAB receptor subunit GB1 at the cell surface independently activates ERK1/2 through IGF-1R transactivation. *PLoS One* **7**, e39698
5. Tu, H., Rondard, P., Xu, C., Bertaso, F., Cao, F., Zhang, X., Pin, J. P., and Liu, J. (2007) Dominant role of GABAB2 and Gbetagamma for GABAB receptor-mediated-ERK1/2/CREB pathway in cerebellar neurons. *Cell Signal* **19**, 1996-2002
6. Tu, H., Xu, C., Zhang, W., Liu, Q., Rondard, P., Pin, J. P., and Liu, J. (2010) GABAB receptor activation protects neurons from apoptosis via IGF-1 receptor transactivation. *J Neurosci* **30**, 749-759
7. Xu, C., Zhang, W., Rondard, P., Pin, J. P., and Liu, J. (2014) Complex GABAB receptor complexes: how to generate multiple functionally distinct units from a single receptor. *Front Pharmacol* **5**, 12
8. Cryan, J., and Kaupmann, K. (2005) A role for GABAB receptors in anxiety and depression. *Trends in pharmacological sciences* **26**, 36-43
9. Cryan, J. F., and Kaupmann, K. (2005) Don't worry 'B' happy!: a role for GABA(B) receptors in anxiety and depression. *Trends in pharmacological sciences* **26**, 36-43
10. Jones, K. A., Borowsky, B., Tamm, J. A., Craig, D. A., Durkin, M. M., Dai, M., Yao, W. J., Johnson, M., Gunwaldsen, C., Huang, L. Y., Tang, C., Shen, Q. R., Salon, J. A., Morse, K., Laz, T., Smith, K. E., Nagarathnam, D., Noble, S. A., Branchek, T. A., and Gerald, C. (1998) GABA(B) receptors function as a heteromeric assembly of the subunits GABA(B)R1 and GABA(B)R2. *Nature* **396**, 674-679
11. White, J. H., Wise, A., Main, M. J., Green, A., Fraser, N. J., Disney, G. H., Barnes, A. A., Emson, P., Foord, S. M., and Marshall, F. H. (1998) Heterodimerization is required for the formation of a functional GABA(B) receptor. *Nature* **396**, 679-682
12. Kaupmann, K., Malitschek, B., Schuler, V., Heid, J., Froest, W., Beck, P., Mosbacher, J., Bischoff, S., Kulik, A., Shigemoto, R., Karschin, A., and Bettler, B. (1998) GABA(B)-receptor subtypes assemble into functional heteromeric complexes. *Nature* **396**, 683-687
13. Kuner, R., Kohr, G., Grunewald, S., Eisenhardt, G., Bach, A., and Kornau, H. C. (1999) Role of heteromer formation in GABAB receptor function. *Science* **283**, 74-77
14. Malitschek, B., Schweizer, C., Keir, M., Heid, J., Froestl, W., Mosbacher, J., Kuhn, R., Henley, J., Joly, C., Pin, J. P., Kaupmann, K., and Bettler, B. (1999) The N-terminal domain of gamma-aminobutyric acid(B) receptors is sufficient to specify agonist and antagonist binding. *Molecular pharmacology* **56**, 448-454
15. Geng, Y., Bush, M., Mosyak, L., Wang, F., and Fan, Q. R. (2013) Structural mechanism of ligand activation in human GABA(B) receptor. *Nature* **504**, 254-259
16. Margeta-Mitrovic, M., Jan, Y. N., and Jan, L. Y. (2001) Function of GB1 and GB2 subunits in

G protein coupling of GABA(B) receptors. *Proceedings of the National Academy of Sciences of the United States of America* **98**, 14649-14654
17. Havlickova, M., Prezeau, L., Duthey, B., Bettler, B., Pin, J.-P., and Blahos, J. (2002) The Intracellular Loops of the GB2 Subunit Are Crucial for G-Protein Coupling of the Heteromeric γ-Aminobutyrate B Receptor. *Molecular pharmacology* **62**, 343
18. Duthey, B., Caudron, S., Perroy, J., Bettler, B., Fagni, L., Pin, J. P., and Prezeau, L. (2002) A single subunit (GB2) is required for G-protein activation by the heterodimeric GABA(B) receptor. *The Journal of biological chemistry* **277**, 3236-3241
19. Couve, A., Filippov, A. K., Connolly, C. N., Bettler, B., Brown, D. A., and Moss, S. J. (1998) Intracellular retention of recombinant GABAB receptors. *The Journal of biological chemistry* **273**, 26361-26367
20. Margeta-Mitrovic, M., Jan, Y. N., and Jan, L. Y. (2000) A trafficking checkpoint controls GABA(B) receptor heterodimerization. *Neuron* **27**, 97-106
21. Pagano, A., Rovelli, G., Mosbacher, J., Lohmann, T., Duthey, B., Stauffer, D., Ristig, D., Schuler, V., Meigel, I., Lampert, C., Stein, T., Prezeau, L., Blahos, J., Pin, J. P., Froestl, W., Kuhn, R., Heid, J., Kaupmann, K., and Bettler, B. (2001) C-terminal interaction is essential for surface trafficking but not for heteromeric assembly of GABA(B) receptors. *Journal of Neuroscience* **21**, 1189-1202
22. Burmakina, S., Geng, Y., Chen, Y., and Fan, Q. R. (2014) Heterodimeric coiled-coil interactions of human GABAB receptor. *Proceedings of the National Academy of Sciences of the United States of America* **111**, 6958-6963
23. Kammerer, R. A., Frank, S., Schulthess, T., Landwehr, R., Lustig, A., and Engel, J. (1999) Heterodimerization of a Functional GABAB Receptor Is Mediated by Parallel Coiled-Coil α-Helices. *Biochemistry-Us* **38**, 13263-13269
24. Calver, A. R., Robbins, M. J., Cosio, C., Rice, S. Q., Babbs, A. J., Hirst, W. D., Boyfield, I., Wood, M. D., Russell, R. B., Price, G. W., Couve, A., Moss, S. J., and Pangalos, M. N. (2001) The C-terminal domains of the GABA(b) receptor subunits mediate intracellular trafficking but are not required for receptor signaling. *J Neurosci* **21**, 1203-1210
25. Mezler, M., Müller, T., and Raming, K. (2001) Cloning and functional expression of GABAB receptors from Drosophila. *European Journal of Neuroscience* **13**, 477-486
26. Hamasaka, Y., Wegener, C., and Nassel, D. R. (2005) GABA modulates Drosophila circadian clock neurons via GABAB receptors and decreases in calcium. *J Neurobiol* **65**, 225-240
27. Gmeiner, F., Kolodziejczyk, A., Yoshii, T., Rieger, D., Nassel, D. R., and Helfrich-Forster, C. (2013) GABA(B) receptors play an essential role in maintaining sleep during the second half of the night in Drosophila melanogaster. *J Exp Biol* **216**, 3837-3843
28. Galvez, T., Duthey, B., Kniazeff, J., Blahos, J., Rovelli, G., Bettler, B., Prézeau, L., and Pin, J. P. (2001) Allosteric interactions between GB1 and GB2 subunits are required for optimal GABA(B) receptor function. *The EMBO journal* **20**, 2152-2159
29. Bass, J., Chiu, G., Argon, Y., and Steiner, D. F. (1998) Folding of insulin receptor monomers is facilitated by the molecular chaperones calnexin and calreticulin and impaired by rapid dimerization. *The Journal of cell biology* **141**, 637-646
30. Terrillon, S., Durroux, T., Mouillac, B., Breit, A., Ayoub, M. A., Taulan, M., Jockers, R., Barberis, C., and Bouvier, M. (2003) Oxytocin and vasopressin V1a and V2 receptors form constitutive homo- and heterodimers during biosynthesis. *Mol Endocrinol* **17**, 677-691

31. Lupas, A., Van Dyke, M., and Stock, J. (1991) Predicting coiled coils from protein sequences. *Science* **252**, 1162-1164
32. Crick, F. H. C. (1953) The packing of α-helices: simple coiled-coils. *Acta Crystallographica* **6**, 689-697
33. Blankenburg, S., Balfanz, S., Hayashi, Y., Shigenobu, S., Miura, T., Baumann, O., Baumann, A., and Blenau, W. (2015) Cockroach GABAB receptor subtypes: molecular characterization, pharmacological properties and tissue distribution. *Neuropharmacology* **88**, 134-144
34. Pregitzer, P., Schultze, A., Raming, K., Breer, H., and Krieger, J. (2013) Expression of a GABA(B) - receptor in olfactory sensory neurons of sensilla trichodea on the male antenna of the moth Heliothis virescens. *Int J Biol Sci* **9**, 707-715
35. Hasegawa, H., Patel, N., Ettehadieh, E., Li, P., and Lim, A. C. (2016) Topogenesis and cell surface trafficking of GPR34 are facilitated by positive-inside rule that effects through a tri-basic motif in the first intracellular loop. *Biochimica et biophysica acta* **1863**, 1534-1551
36. Boyd, G. W., Doward, A. I., Kirkness, E. F., Millar, N. S., and Connolly, C. N. (2003) Cell surface expression of 5-hydroxytryptamine type 3 receptors is controlled by an endoplasmic reticulum retention signal. *The Journal of biological chemistry* **278**, 27681-27687
37. Cunningham, M. R., McIntosh, K. A., Pediani, J. D., Robben, J., Cooke, A. E., Nilsson, M., Gould, G. W., Mundell, S., Milligan, G., and Plevin, R. (2012) Novel role for proteinase-activated receptor 2 (PAR2) in membrane trafficking of proteinase-activated receptor 4 (PAR4). *The Journal of biological chemistry* **287**, 16656-16669
38. Brock, C., Boudier, L., Maurel, D., Blahos, J., and Pin, J. P. (2005) Assembly-dependent surface targeting of the heterodimeric GABA(B) receptor is controlled by COPI but not 14-3-3. *Molecular Biology of the Cell* **16**, 5572-5578
39. Restituito, S., Couve, A., Bawagan, H., Jourdain, S., Pangalos, M. N., Calver, A. R., Freeman, K. B., and Moss, S. J. (2005) Multiple motifs regulate the trafficking of GABA(B) receptors at distinct checkpoints within the secretory pathway. *Molecular and Cellular Neuroscience* **28**, 747-756
40. Doly, S., Shirvani, H., Gata, G., Meye, F. J., Emerit, M. B., Enslen, H., Achour, L., Pardo-Lopez, L., Yang, S. K., Armand, V., Gardette, R., Giros, B., Gassmann, M., Bettler, B., Mameli, M., Darmon, M., and Marullo, S. (2015) GABA receptor cell-surface export is controlled by an endoplasmic reticulum gatekeeper. *Molecular psychiatry*
41. Li, C., Zhao, X., Cao, X., Chu, D., Chen, J., and Zhou, J. (2008) The Drosophila homolog of jwa is required for ethanol tolerance. *Alcohol Alcohol* **43**, 529-536
42. Grieder, N. C., Kloter, U., and Gehring, W. J. (2005) Expression of COPI components during development of Drosophila melanogaster. *Gene Expr Patterns* **6**, 11-21
43. Fuss, B., Becker, T., Zinke, I., and Hoch, M. (2006) The cytohesin Steppke is essential for insulin signalling in Drosophila. *Nature* **444**, 945-948
44. Prosser, H. M., Gill, C. H., Hirst, W. D., Grau, E., Robbins, M., Calver, A., Soffin, E. M., Farmer, C. E., Lanneau, C., Gray, J., Schenck, E., Warmerdam, B. S., Clapham, C., Reavill, C., Rogers, D. C., Stean, T., Upton, N., Humphreys, K., Randall, A., Geppert, M., Davies, C. H., and Pangalos, M. N. (2001) Epileptogenesis and enhanced prepulse inhibition in GABA(B1)-deficient mice. *Mol Cell Neurosci* **17**, 1059-1070
45. Schuler, V., Lüscher, C., Blanchet, C., Klix, N., Sansig, G., Klebs, K., Schmutz, M., Heid, J., Gentry, C., Urban, L., Fox, A., Spooren, W., Jaton, A.-L., Vigouret, J.-M., Pozza, M., Kelly, P.

H., Mosbacher, J., Froestl, W., Käslin, E., Korn, R., Bischoff, S., Kaupmann, K., van der Putten, H., and Bettler, B. (2001) Epilepsy, Hyperalgesia, Impaired Memory, and Loss of Pre- and Postsynaptic GABAB Responses in Mice Lacking GABAB(1). *Neuron* **31**, 47-58

46. Rondard, P., Huang, S., Monnier, C., Tu, H., Blanchard, B., Oueslati, N., Malhaire, F., Li, Y., Trinquet, E., Labesse, G., Pin, J. P., and Liu, J. (2008) Functioning of the dimeric GABA(B) receptor extracellular domain revealed by glycan wedge scanning. *The EMBO journal* **27**, 1321-1332
47. Xue, L., Sun, Q., Zhao, H., Rovira, X., Gai, S., He, Q., Pin, J. P., Liu, J., and Rondard, P. (2019) Rearrangement of the transmembrane domain interfaces associated with the activation of a GPCR hetero-oligomer. *Nature communications* **10**, 2765
48. Ikura, M., Kay, L. E., and Bax, A. (1990) A novel approach for sequential assignment of 1H, 13C, and 15N spectra of proteins: heteronuclear triple-resonance three-dimensional NMR spectroscopy. Application to calmodulin. *Biochemistry-Us* **29**, 4659-4667
49. Bax, A., Ikura, M., Kay, L. E., Barbato, G., and Spera, S. (1991) Multidimensional triple resonance NMR spectroscopy of isotopically uniformly enriched proteins: a powerful new strategy for structure determination. *Ciba Found Symp* **161**, 108-119; discussion 119-135
50. Bax, A., and Ikura, M. (1991) An efficient 3D NMR technique for correlating the proton and 15N backbone amide resonances with the alpha-carbon of the preceding residue in uniformly 15N/13C enriched proteins. *Journal of biomolecular NMR* **1**, 99-104
51. Delaglio, F., Grzesiek, S., Vuister, G. W., Zhu, G., Pfeifer, J., and Bax, A. (1995) NMRPipe: a multidimensional spectral processing system based on UNIX pipes. *Journal of biomolecular NMR* **6**, 277-293
52. Vranken, W. F., Boucher, W., Stevens, T. J., Fogh, R. H., Pajon, A., Llinas, M., Ulrich, E. L., Markley, J. L., Ionides, J., and Laue, E. D. (2005) The CCPN data model for NMR spectroscopy: development of a software pipeline. *Proteins* **59**, 687-696
53. Brunger, A. T., Adams, P. D., Clore, G. M., DeLano, W. L., Gros, P., Grosse-Kunstleve, R. W., Jiang, J. S., Kuszewski, J., Nilges, M., Pannu, N. S., Read, R. J., Rice, L. M., Simonson, T., and Warren, G. L. (1998) Crystallography & NMR system: A new software suite for macromolecular structure determination. *Acta Crystallogr D Biol Crystallogr* **54**, 905-921
54. Brunger, A. T. (2007) Version 1.2 of the Crystallography and NMR system. *Nature protocols* **2**, 2728-2733
55. Rieping, W., Habeck, M., Bardiaux, B., Bernard, A., Malliavin, T. E., and Nilges, M. (2007) ARIA2: automated NOE assignment and data integration in NMR structure calculation. *Bioinformatics* **23**, 381-382
56. Cheung, M. S., Maguire, M. L., Stevens, T. J., and Broadhurst, R. W. (2010) DANGLE: A Bayesian inferential method for predicting protein backbone dihedral angles and secondary structure. *J Magn Reson* **202**, 223-233

Figure 1

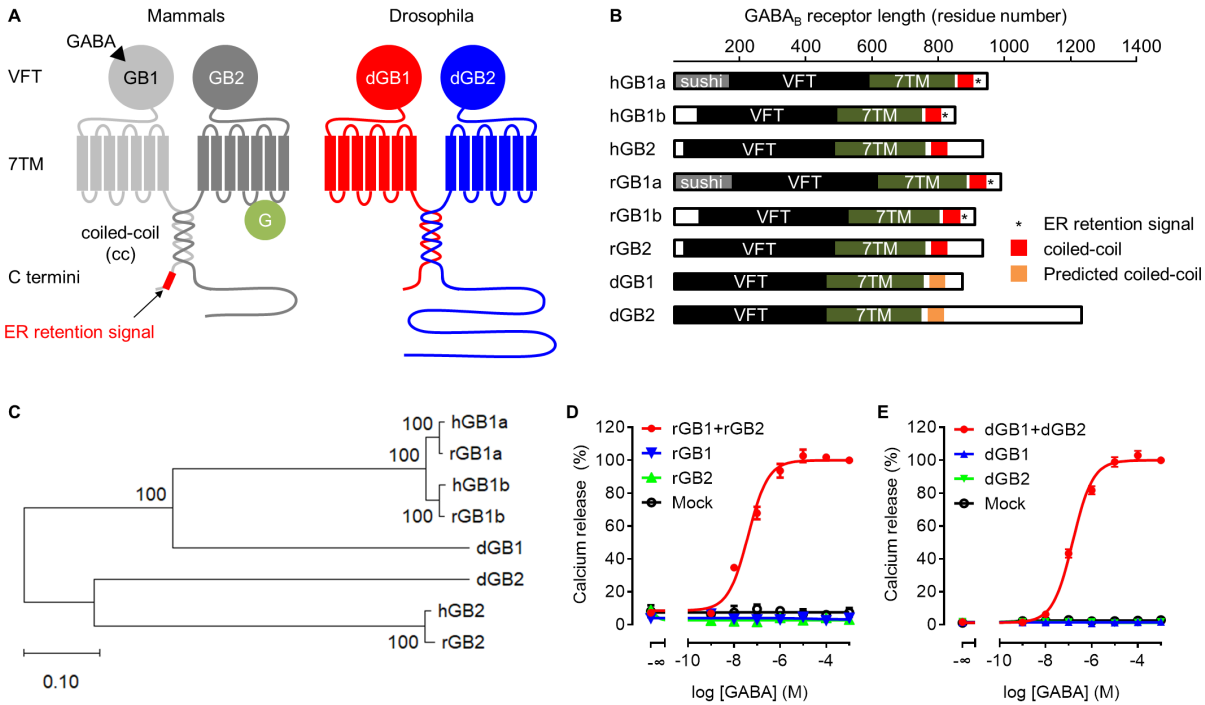
A
Mammals
Drosophila
GABA
VFT
GB1
GB2
dGB1
dGB2
7TM
G
coiled-coil
(cc)
C termini
ER retention signal
B
GABA$_B$ receptor length (residue number)
200
400
600
800
1000
1200
1400
hGB1a
hGB1b
hGB2
rGB1a
rGB1b
rGB2
dGB1
dGB2
sushi
VFT
7TM
* ER retention signal
coiled-coil
Predicted coiled-coil
C
100
hGB1a
rGB1a
hGB1b
rGB1b
dGB1
dGB2
hGB2
rGB2
0.10
D
rGB1+rGB2
rGB1
rGB2
Mock
Calcium release (%)
log [GABA] (M)
E
dGB1+dGB2
dGB1
dGB2
Mock
Calcium release (%)
log [GABA] (M)

Figure 1. Comparison of *drosophila* and mammalian $GABA_B$ receptors. (A) Schematic representation of mammalian $GABA_B$ made of the two obligatory subunits GB1 and GB2 where GB1 binds the GABA in the Venus flytrap domain (VFT) while GB2 couples to the G protein through its seven transmembrane domain (7TM). A similar organization is expected for the drosophila $GABA_B$ receptor, with the two subunits dGB1 and dGB2. In mammalian receptors, the R-x-R ER retention signal is masked by the coiled-coil (cc) domain formed by the proximal C-terminal regions of GB1 and GB2, allowing trafficking of the heterodimer to the cell surface. Such trafficking remains unknown for the drosophila $GABA_B$. **(B)** Subdomain organization of human, rat and *drosophila* $GABA_B$ receptor subunits with the two most common isoforms GB1a and GB1b for the mammalian GB1 subunits. The length of receptor indicates the number of amino acids. In human (h) and rat (r) $GABA_B$ receptor, sushi domain (dark gray in the N-terminus of GB1a), VFT (black) and 7TM (olive) domains, cc region (red) and R-x-R ER retention motif (asterisk) are shown. Drosophila predicted cc region (orange) is indicated. **(C)** Phylogenetic analysis of the indicated human, rat and *drosophila* $GABA_B$ receptor subunits, using the neighbor-joining method. The genetic distances are calculated with MEGA X. The numbers at the nodes of the branches represent the percentage of bootstrap test (1000 replicates). Scale bar, 0.1 = 10 % genetic distance. **(D-E)** Intracellular calcium release induced by GABA in HEK-293 cells co-transfected with either rat or *drosophila* $GABA_B$ receptor as indicated, and chimeric G protein Gqi_9. Normalized data are mean ± SEM (N=3 experiments).

Figure 2

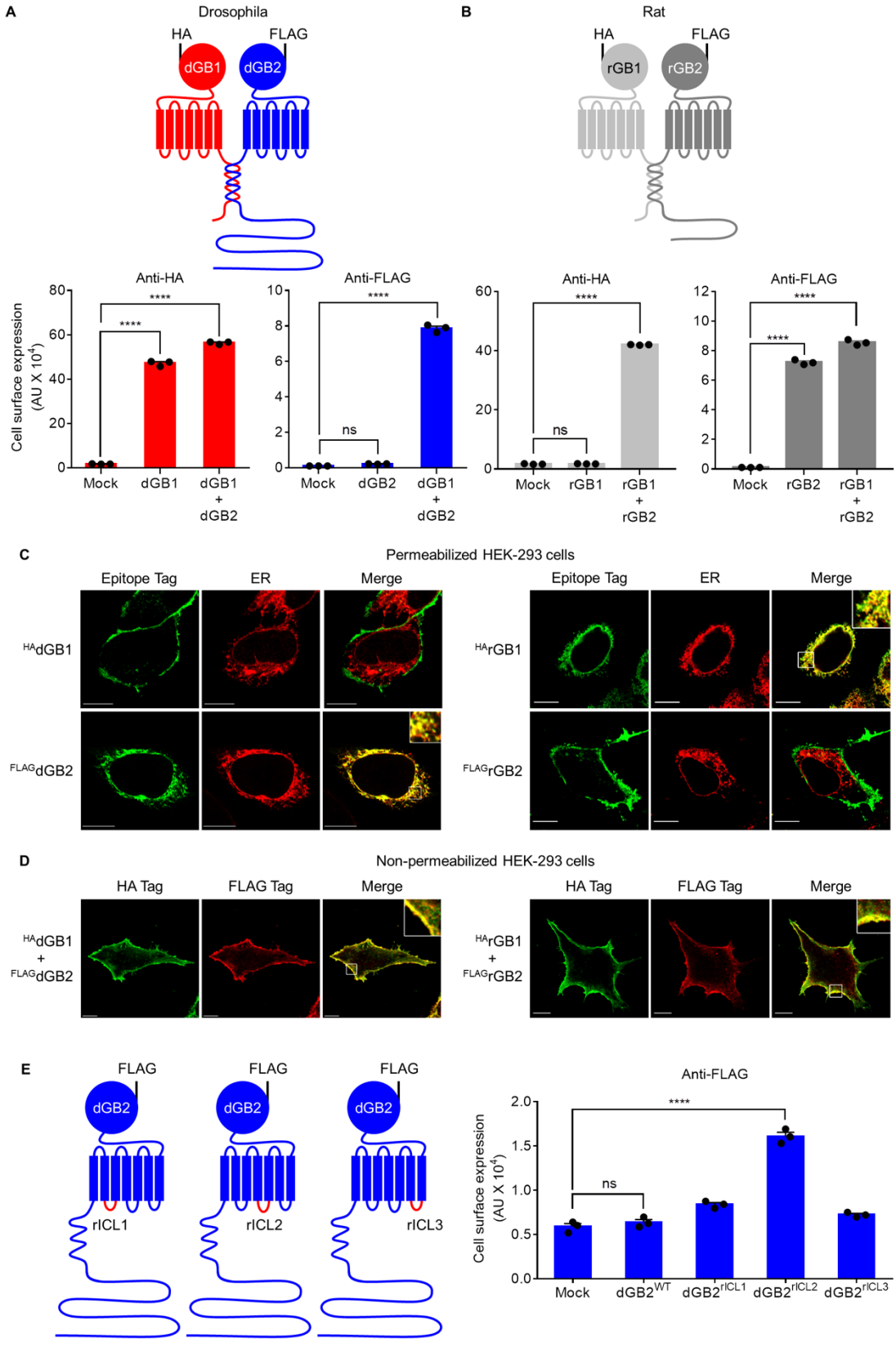
A
Drosophila
HA
FLAG
dGB1
dGB2
Anti-HA
Anti-FLAG
Cell surface expression (AU X 10⁴)
Mock
dGB1
dGB1 + dGB2
dGB2
ns
****
B
Rat
rGB1
rGB2
rGB1 + rGB2
C
Permeabilized HEK-293 cells
Epitope Tag
ER
Merge
HAdGB1
FLAGdGB2
HArGB1
FLAGrGB2
D
Non-permeabilized HEK-293 cells
HA Tag
FLAG Tag
HAdGB1 + FLAGdGB2
HArGB1 + FLAGrGB2
E
rICL1
rICL2
rICL3
dGB2WT
dGB2rICL1
dGB2rICL2
dGB2rICL3

Figure 2. Cell surface expression of *drosophila* and rat $GABA_B$ subunits. (A-B), ELISA measurement of the amount of indicated HA-tagged GB1 and Flag-tagged GB2 at the cell surface when expressed alone or co-expressed with the other subunits. dGB1 (red), dGB2 (blue), rGB1 (light gray) and rGB2 (dark gray). Data represent the means ± SEM from 3 independent experiments, one-way ANOVA test. ns, non significance; **** $p<0.0001$. **(C)** Fluorescent detection of the indicated HA-tagged GB1 and FLAG-tagged GB2 subunits expressed alone from fixed and permeabilized HEK-293 cells. dGB2 and rGB1 overlapped with the ER marker calreticulin (93.1 ± 2.3 % and 92.0 ± 1.3 % respectively), but not dGB1 and rGB2 (2.8 ± 1.0 % and 1.3 ± 0.6 % respectively). These results mean ± SEM from three independent experiments. Scale bar, 10 µm. Insets: enlarged areas as indicated (white square). **(D)** Fluorescent detection of the indicated HA-tagged GB1 and FLAG-tagged GB2 subunits co-expressed from fixed but non-permeabilized cells. dGB2 overlapped (merge panels) with dGB1 (95.4 ± 1.7 %) and rGB1 with rGB2 (97.0 ± 1.1 %). These results mean ± SEM from three independent experiments. Scale bar, 10 µm. Insets: enlarged areas as indicated. **(E)** ELISA measurement of the amount of indicated FLAG-tagged dGB2 constructs at the cell surface when expressed alone. rICL1, rICL2 and rICL3 indicated the three intracellular regions of rat GB2 that were replaced in dGB2. Data represent the means ± SEM from 3 independent experiments, one-way ANOVA test. ns, non significance, **** $p<0.0001$.

Figure 3

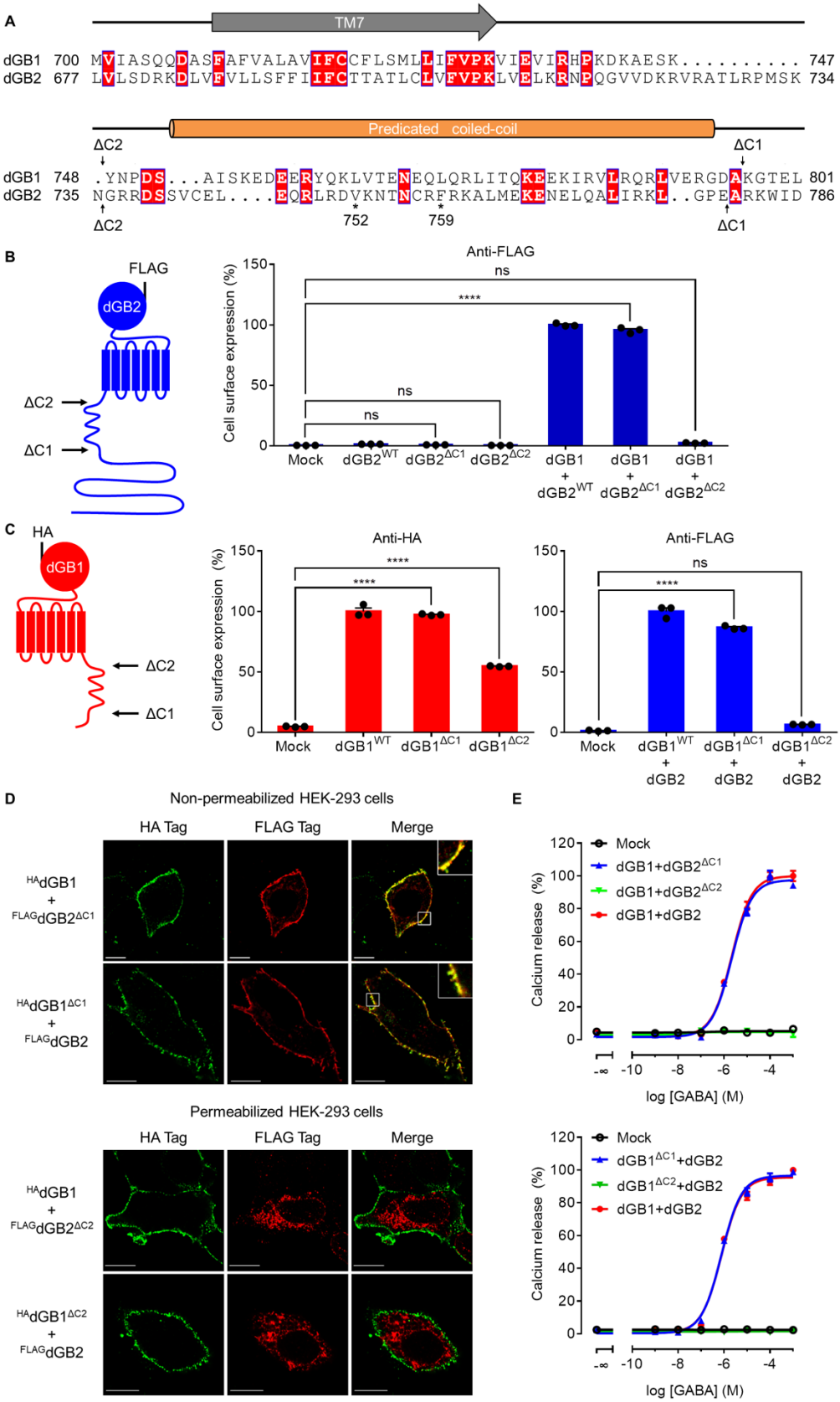
A
TM7
dGB1 700 MVIASQQDASFAFVALAVIFCCFLSMLLIFVPKVIEVIRHPKDKAESK..... 747
dGB2 677 LVLSDRKDLVFVLLSFFIIFCTTATLCLVFVPKLVELKRNPQGVVDKRVRATLRPMSK 734
Predicated coiled-coil
ΔC2
ΔC1
dGB1 748 .YNPDS...AISKEDEERYQKLVTENEQLQRLITQKEEKIRVLRQRLVERGDAKGTEL 801
dGB2 735 NGRRDSSVCEL....EQRLRDVKNTNCRFRKALMEKENELQALIRKL..GPEARKWID 786
752
759
B
FLAG
dGB2
Anti-FLAG
Cell surface expression (%)
Mock
dGB2WT
dGB2ΔC1
dGB2ΔC2
dGB1 + dGB2WT
dGB1 + dGB2ΔC1
dGB1 + dGB2ΔC2
ns
****
C
HA
dGB1
Anti-HA
Anti-FLAG
dGB1WT
dGB1ΔC1
dGB1ΔC2
dGB1WT + dGB2
dGB1ΔC1 + dGB2
dGB1ΔC2 + dGB2
D
Non-permeabilized HEK-293 cells
HA Tag
FLAG Tag
Merge
HAdGB1 + FLAGdGB2ΔC1
HAdGB1ΔC1 + FLAGdGB2
Permeabilized HEK-293 cells
HAdGB1 + FLAGdGB2ΔC2
HAdGB1ΔC2 + FLAGdGB2
E
Mock
dGB1+dGB2ΔC1
dGB1+dGB2ΔC2
dGB1+dGB2
dGB1ΔC1+dGB2
dGB1ΔC2+dGB2
Calcium release (%)
log [GABA] (M)

Figure 3. **Coiled-coil domain controls cell surface trafficking of *drosophila* $GABA_B$ receptor. (A)** Sequence alignments of the proximal C-terminal region of dGB1 and dGB2 with Clustal Omega and displayed by ESPript 3 (http://espript.ibcp.fr/ESPript/cgi-bin/ESPript.cgi). ΔC1 and ΔC2 indicate the position of the truncatures of dGB1 and dGB2. 7^{th} transmembrane helix (TM7) and the predicted coiled-coil regions are indicated. **(B-C)** ELISA measurement of the amount of the wild-type (WT) subunits and the indicated HA-tagged GB1 and Flag-tagged GB2 constructs at the cell surface when expressed alone or co-expressed with the other subunits. Data represent the means ± SEM from 3 independent experiments, one-way ANOVA test, ns: non significance, **** $p<0.0001$. **(D)** Fluorescent detection of the indicated HA-tagged GB1 and FLAG-tagged GB2 constructs co-expressed from fixed and permeabilized or non-permeabilized cells. $dGB2^{\Delta C1}$ overlapped with dGB1 (97.0 ± 1.1 %), dGB2 with $dGB1^{\Delta C1}$ (80.2 ± 6.7 %), but not $dGB2^{\Delta C2}$ with dGB1 (3.9 ± 1.9 %) and dGB2 with $dGB1^{\Delta C2}$ (2.4 ± 0.4 %). These results mean ± SEM from three independent experiments. Scale bar, 10 μm. Insets, enlarged areas as indicated. **(E)** Intracellular calcium release induced by GABA in cells co-transfected with the indicated constructs. Normalized data are mean ± SEM (N=3 experiments).

Figure 4

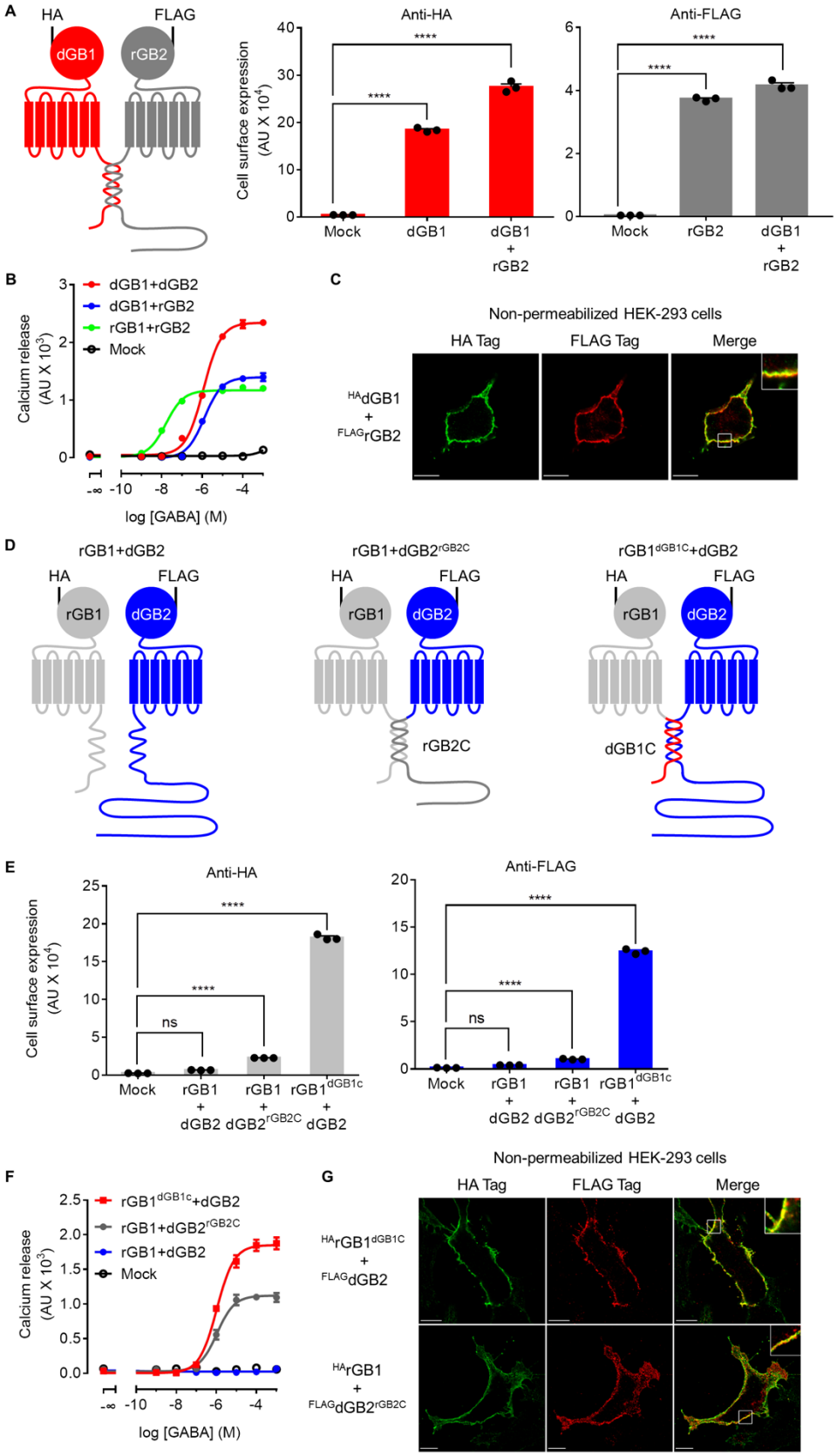
A
HA
FLAG
dGB1
rGB2
Anti-HA
Anti-FLAG
Cell surface expression (AU X 10^4)
****
Mock
dGB1
dGB1 + rGB2
rGB2
B
dGB1+dGB2
dGB1+rGB2
rGB1+rGB2
Mock
Calcium release (AU X 10^3)
log [GABA] (M)
C
Non-permeabilized HEK-293 cells
HA Tag
FLAG Tag
Merge
HAdGB1 + FLAGrGB2
D
rGB1+dGB2
rGB1+dGB2rGB2C
rGB1dGB1C+dGB2
rGB1
dGB2
rGB2C
dGB1C
E
Anti-HA
Anti-FLAG
ns
rGB1 + dGB2
rGB1 + dGB2rGB2C
rGB1dGB1c + dGB2
F
rGB1dGB1c+dGB2
rGB1+dGB2rGB2C
rGB1+dGB2
Mock
Calcium release (AU X 10^3)
log [GABA] (M)
G
Non-permeabilized HEK-293 cells
HA Tag
FLAG Tag
Merge
HArGB1dGB1C + FLAGdGB2
HArGB1 + FLAGdGB2rGB2C

Figure 4. Drosophila coiled-coil interaction is highly specific. (A) ELISA measurement of the amount of the wild-type indicated HA-tagged GB1 and Flag-tagged GB2 constructs at the cell surface when expressed alone or co-expressed with the other subunits. Cell surface expression was measured by ELISA. Data represent the means ± SEM from 3 independent experiments, one-way ANOVA test, ns: non significance, **** p<0.0001. **(B)** Intracellular calcium release induced by GABA in cells co-transfected with the indicated constructs. Data are mean ± SEM from a typical experiment performed three times. **(C)** Fluorescent detection of HA-tagged dGB1 co-expressed with FLAG-tagged rGB2 (77.2 ± 3.3 % overlapping) from non-permeabilized cells. These results mean ± SEM from three independent experiments. Scale bar, 10 µm. Inset, enlarged areas as indicated. **(D-E)** Schematic representation of the constructs HA-tagged rGB1 and FLAG-tagged dGB2, and ELISA measurement of their amount at the cell surface when co-expressed. Cell surface expression was measured by ELISA. Data represent the means ± SEM from 3 independent experiments, one-way ANOVA test, ns, non significance, **** p<0.0001. **(F)** Intracellular calcium release induced by GABA in cells co-transfected with the indicated constructs. Data are mean ± SEM from a typical experiment performed three times. **(G)** Fluorescent detection of the HA-tagged rGB1 constructs co-expressed with the FLAG-tagged dGB2 constructs from non-permeabilized cells. $rGB1^{dGB1C}$ overlapped with dGB2 (78.0 ± 4.4 %), and rGB1 with $dGB2^{rGB2C}$ (84.1 ± 4.9 %). These results mean ± SEM from three independent experiments. Scale bar, 10 µm. Insets, enlarged areas as indicated.

Figure 5

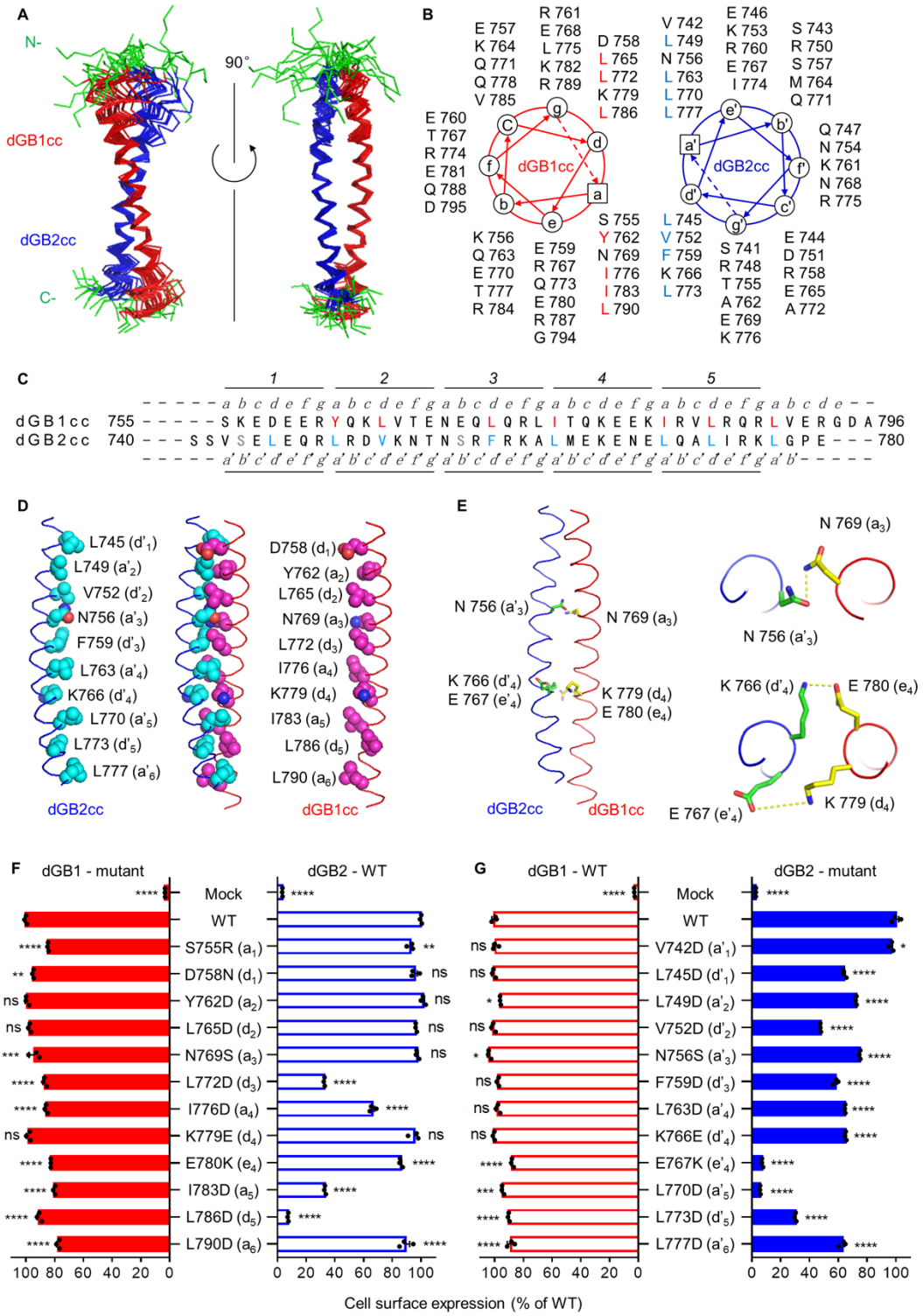
A
N-
dGB1cc
dGB2cc
C-
90°
B
dGB1cc
dGB2cc
C
dGB1cc 755 S K E D E E R Y Q K L V T E N E Q L Q R L I T Q K E E K I R V L R Q R L V E R G D A 796
dGB2cc 740 S S V S E L E Q R L R D V K N T N S R F R K A L M E K E N E L Q A L I R K L G P E 780
D
L745 (d'1)
L749 (a'2)
V752 (d'2)
N756 (a'3)
F759 (d'3)
L763 (a'4)
K766 (d'4)
L770 (a'5)
L773 (d'5)
L777 (a'6)
dGB2cc
D758 (d1)
Y762 (a2)
L765 (d2)
N769 (a3)
L772 (d3)
I776 (a4)
K779 (d4)
I783 (a5)
L786 (d5)
L790 (a6)
dGB1cc
E
N 756 (a'3)
N 769 (a3)
K 766 (d'4)
E 767 (e'4)
K 779 (d4)
E 780 (e4)
dGB2cc
dGB1cc
N 769 (a3)
N 756 (a'3)
K 766 (d'4)
E 780 (e4)
E 767 (e'4)
K 779 (d4)
F
dGB1 - mutant
dGB2 - WT
Mock
WT
S755R (a1)
D758N (d1)
Y762D (a2)
L765D (d2)
N769S (a3)
L772D (d3)
I776D (a4)
K779E (d4)
E780K (e4)
I783D (a5)
L786D (d5)
L790D (a6)
G
dGB1 - WT
dGB2 - mutant
Mock
WT
V742D (a'1)
L745D (d'1)
L749D (a'2)
V752D (d'2)
N756S (a'3)
F759D (d'3)
L763D (a'4)
K766E (d'4)
E767K (e'4)
L770D (a'5)
L773D (d'5)
L777D (a'6)
Cell surface expression (% of WT)

Figure 5. Structural analysis of *drosophila* $GABA_B$ receptor coiled-coil domain. (A) Backbone heavy atom superimposition of the 20 generated cc solution structures. Structures were aligned by well-defined α-helical residues. dGB1cc (red), dGB2cc (blue), flexible residues of the N- and C-terminal end (green) are shown. **(B)** Helical wheel alignment of the residues in the heterodimeric cc complex. The view is from the N termini of dGB1cc and dGB2cc. **(C)** Protein sequences aligment of the dGB1cc and dGB2cc regions. Five completed canonical heptad repeats and residues in cc from position *a* to *g* or *a'* to *g'* of are labeled. Hydrophobic residues in the interface of dGB1cc (red) and dGB2cc (blue) are shown. **(D)** The "knobs" were shown using a sphere representation for each individual chain with the contact surface facing the viewer, and as a complex. Residue number and position in helical wheel are labeled. **(E)** Both the hydrogen bond interaction between the indicated and conserved Asn pair and the pair of salt bridges are highlighted in the structure of the cc domain and in enlarged views. **(F-G)** ELISA measurement of the amount of the wild-type HA-tagged dGB1 and Flag-tagged dGB2 at the cell surface when co-expressed with the indicated mutated subunits. Data represent the means ± SEM from 3 independent experiments, one-way ANOVA test, ns, non significance, * $p<0.05$, ** $p<0.01$, *** $p<0.001$, **** $p<0.0001$.

Figure 6

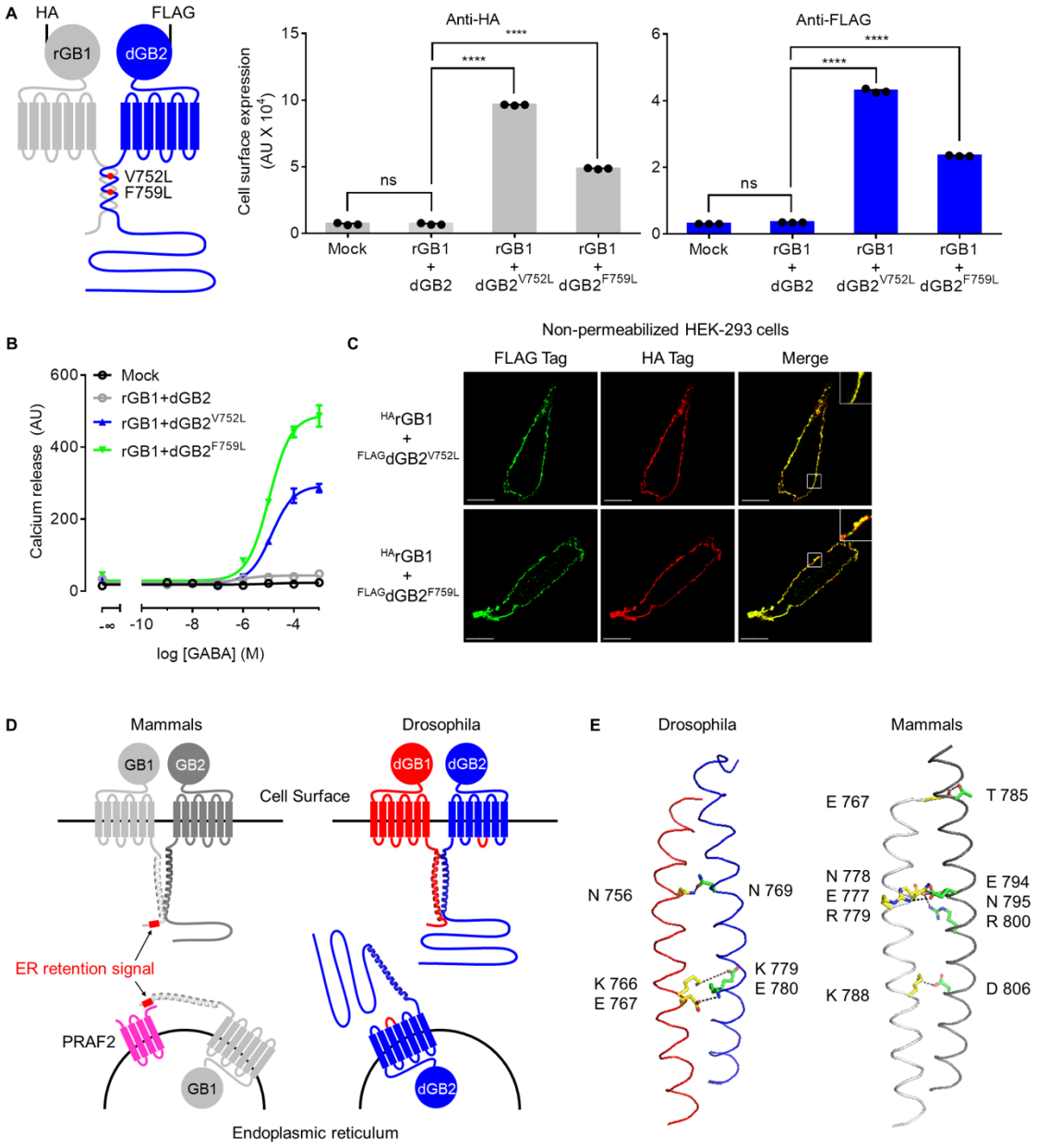
A
HA
FLAG
rGB1
dGB2
V752L
F759L
Anti-HA
Anti-FLAG
Cell surface expression (AU X 10^4)
ns
****
Mock
rGB1 + dGB2
rGB1 + dGB2^V752L
rGB1 + dGB2^F759L
B
Mock
rGB1+dGB2
rGB1+dGB2^V752L
rGB1+dGB2^F759L
Calcium release (AU)
log [GABA] (M)
C
Non-permeabilized HEK-293 cells
FLAG Tag
HA Tag
Merge
HArGB1 + FLAGdGB2^V752L
HArGB1 + FLAGdGB2^F759L
D
Mammals
Drosophila
GB1
GB2
dGB1
dGB2
Cell Surface
ER retention signal
PRAF2
Endoplasmic reticulum
E
Drosophila
Mammals
N 756
N 769
K 766
E 767
K 779
E 780
E 767
T 785
N 778
E 777
R 779
E 794
N 795
R 800
K 788
D 806

Figure 6. Highly conserved coiled-coil domain interaction for a functional $GABA_B$ heterodimer. **(A)** ELISA measurement of the amount of the indicated FLAG-tagged dGB2 mutated in the cc domain, at the cell surface co-expressed with the wild-type rGB1, and of HA-tagged wild-type rGB1 in the same experiments. Data represent the means ± SEM from three independent experiments, one-way ANOVA test. ns, non significance, **** $p<0.0001$. **(B)** Intracellular calcium release induced by GABA in cells co-transfected with the wild-type or mutants dGB2 coexpressed with wild-type rGB1. Data are mean ± SEM from a typical experiment performed three times. **(C)** Fluorescent detection of the wild-type HA-tagged rGB1 co-expressed with the indicated FLAG-tagged dGB2 mutants. rGB1 overlapped with $dGB2^{V752L}$ (87.5 ± 0.6 %) and $dGB2^{F759L}$ (88.0 ± 0.3 %). These results mean ± SEM from three independent experiments. Scale bar, 10 µm. Insets, enlarged areas as indicated. **(D)** In mammalian, GB1 is intracellularly retained due to its RSRR motif that interacts with the ER chaperone PRAF2 (40), while GB2 facilitates its release through the cc interaction producing a steric hindrance for PRAF2 interaction and then allowing the cell surface trafficking of the heterodimer. In contrast, drosophila dGB2 is retained in ER through an unknown mechanism, probably through molecular determinants located inside ICL2 (red). Interaction of dGB1 with dGB2 leads to the cell surface trafficking of the heterodimer through a conserved cc interaction. **(E)** Comparison of the structures of the cc domain for the drosophila and mammal (PDB code 4PAS) $GABA_B$ receptor, solved in the present study and previously reported (22), respectively. The polar and charged-charged interactions are shown. Of note, the sequences of the cc regions are identical in mammals (human, rat and mouse).

Supplementary Information

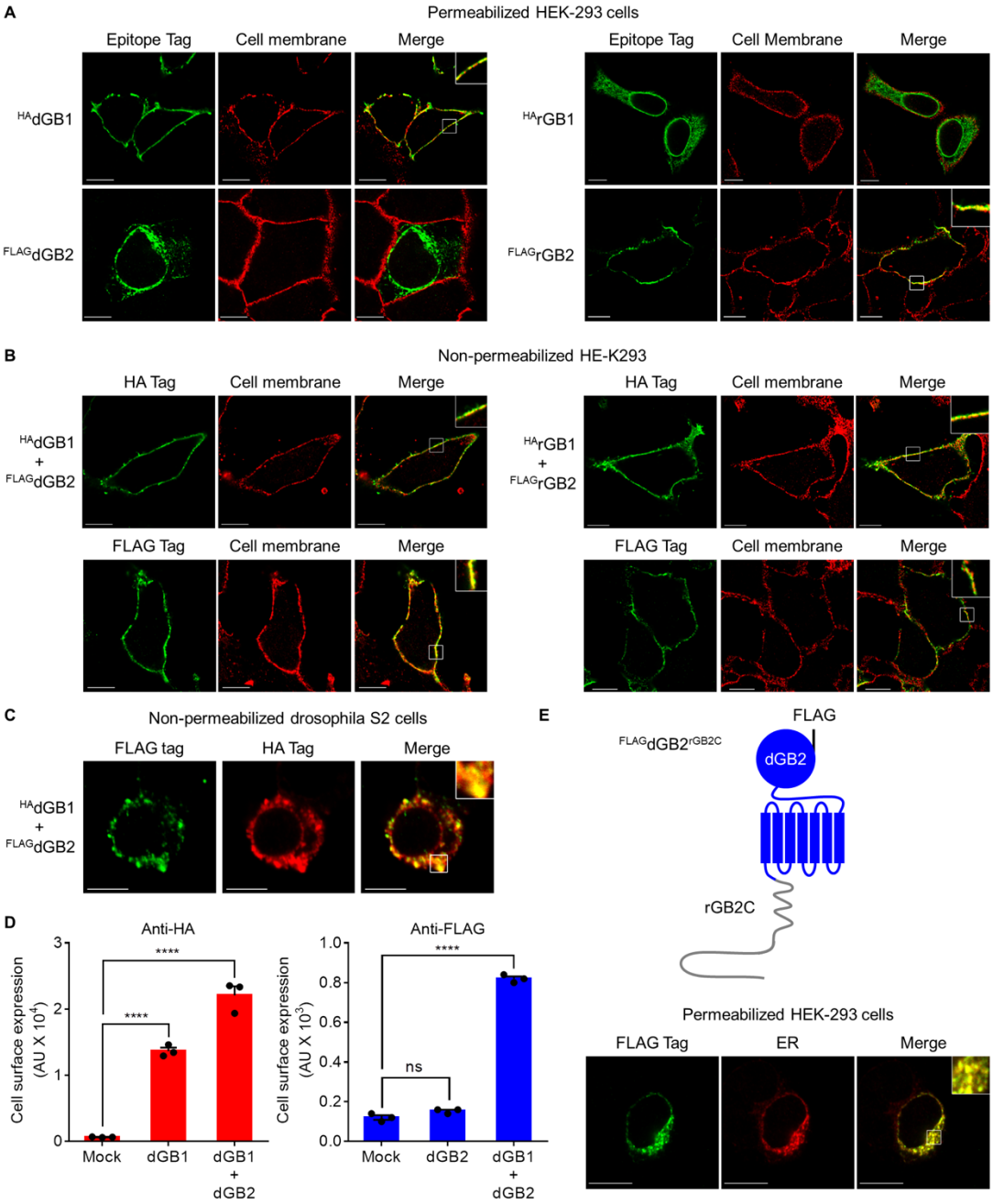

Figure S1. Cell surface expression of rat and drosophila $GABA_B$ receptor. (A) Fluorescent detection of the indicated HA-tagged GB1 and FLAG-tagged GB2 subunits expressed alone, and the Na,K-ATPase α_1 subunit, from fixed and permeabilized HEK-293 cells. dGB1 and rGB2 overlapped with the cell membrane marker Na,K-ATPase α_1 (76.2 ± 5.8 % and 76.0 ± 3.0 %, respectively), but not rGB1 and dGB2 (5.0 ± 0.3 %, 3.5 ± 0.6 % respectively). **(B)** Fluorescent detection of drosophila or rat HA-tagged GB1 and FLAG-tagged GB2 subunits co-expressed, and Na,K-ATPase α_1, from non-permeabilized HEK-293 cells. dGB1, dGB2, rGB1 and rGB2 overlapped with Na,K-ATPase α_1 (79.0 ± 4.0 %, 80.5 ± 3.4 %, 73.2 ± 5.2 % and 68.4 ± 4.9 %, respectively). **(C)** Fluorescent detection of the HA-tagged dGB1 and FLAG-tagged dGB2 when co-expressed from non-permeabilized drosophila S2 cells. dGB2 overlapped with dGB1 (82.7 ± 2.6 %). **(D)** ELISA measurement of the amount of HA-tagged dGB1 and Flag-tagged dGB2 at the cell surface when expressed alone or co-expressed with the other subunits. Data represent the means ± SEM from three independent experiments, one-way ANOVA test. ns, non significance, **** $p<0.0001$. **(E)** Fluorescent detection of the indicated FLAG-dGB2 construct expressed alone, and the calreticulin, from permeabilized HEK-293 cells (95.1 ± 2.2 % overlapping). Of note, in panel A-C and E, values indicate the mean ± SEM from three independent experiments. Scale bar, 10 μm. Insets: enlarged areas as indicated.

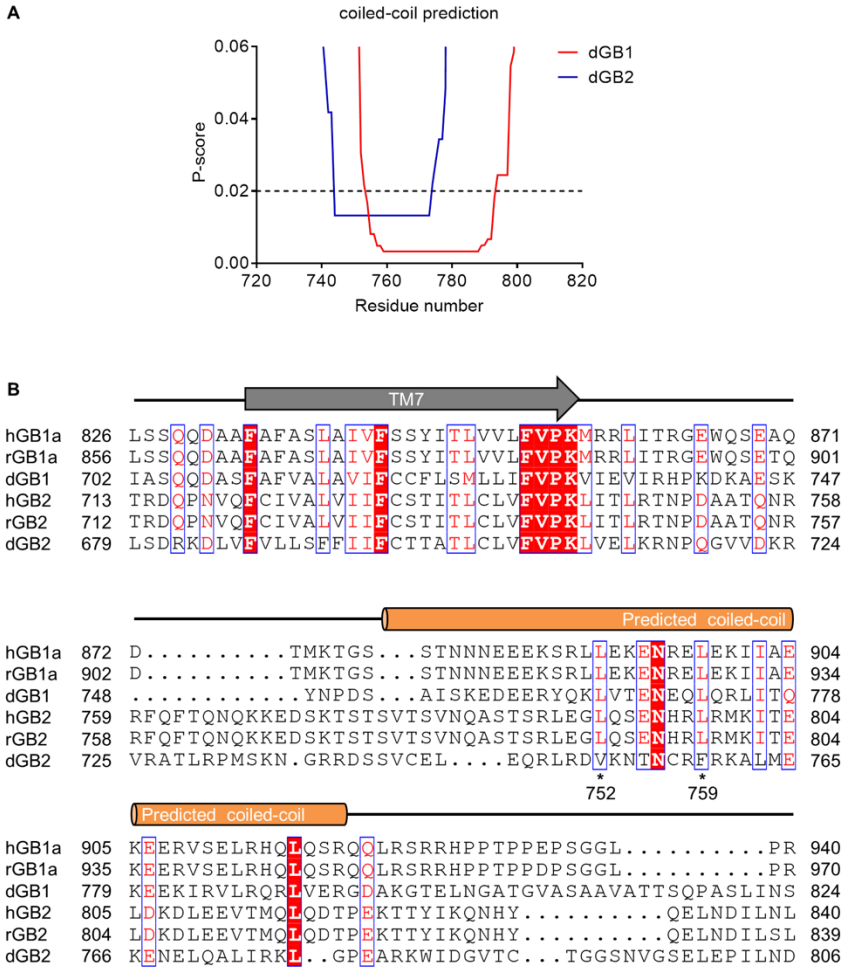

Figure S2. Coiled-coil domain prediction of the drosophila $GABA_B$ receptor subunits. (A) The algorithm COILS predicts a coil-coiled structure for the regions 740-780 and 750-800 of dGB1 and dGB2, respectively (P-score below 0.02). **(B)** Protein sequence alignments of human, rat and drosophila $GABA_B$ subunits, generated by Clustal Omega and displayed by ESPript 3. The 7th transmembrane helix and predicted coiled-coil regions are shown.

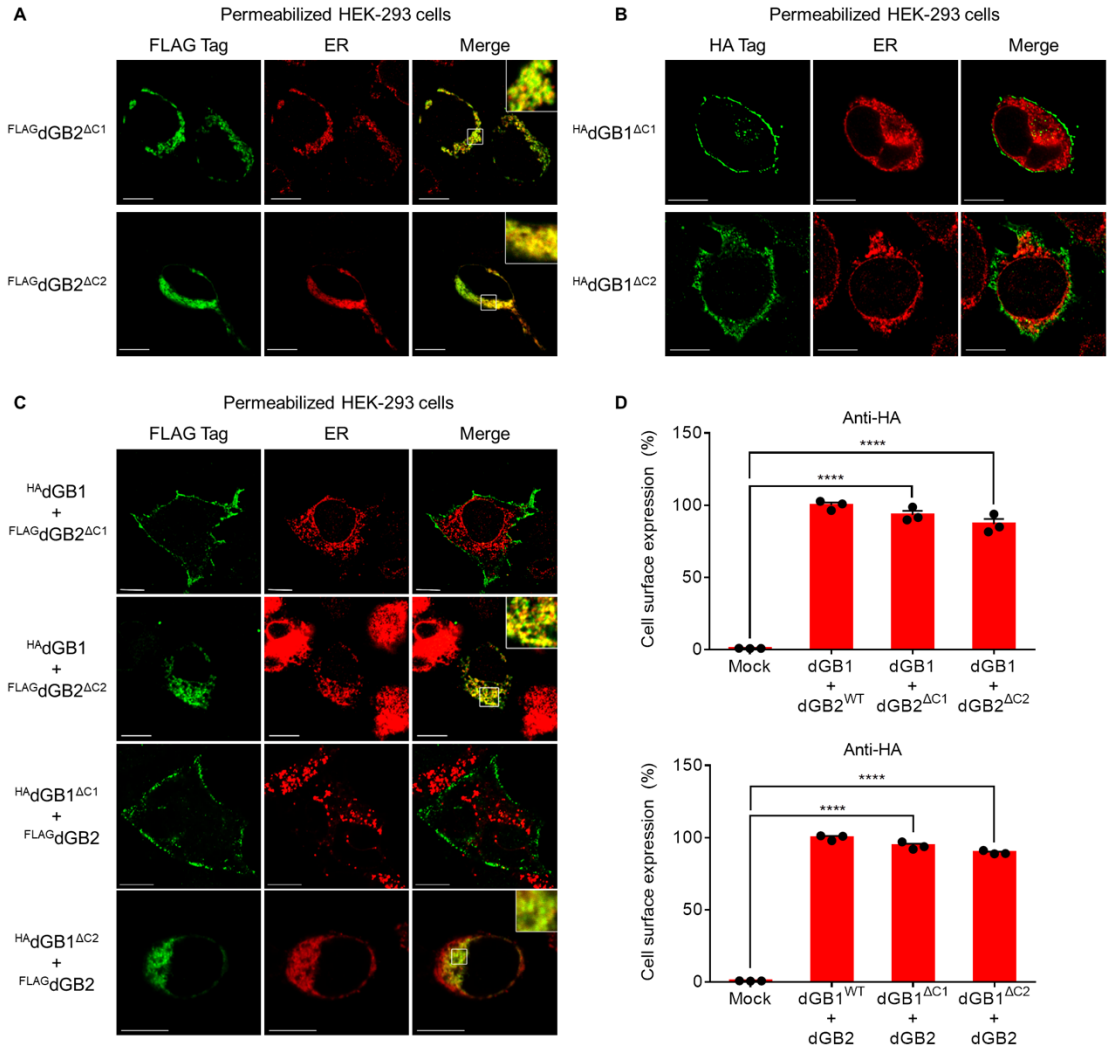

Figure S3. **Coiled-coil interaction controls cell surface trafficking of drosophila $GABA_B$ receptor.** **(A-B)** Fluorescent detection of the indicated HA-tagged GB1 and FLAG-tagged GB2 constructs when expressed alone or co-expressed, and of calreticulin, from permeabilized HEK-293 cells. $dGB2^{\Delta C1}$ and $dGB2^{\Delta C2}$ overlapped with calreticulin (93.2 ± 4.0 % and 95.4 ± 1.6 % respectively), but not $dGB1^{\Delta C1}$ and $dGB1^{\Delta C2}$ (5.8 ± 1.6 % and 5.2 ± 1.7 %, respectively). **(C and E)** Fluorescent detection of the indicated HA-tagged dGB1 and FLAG-tagged dGB2 constructs co-expressed from permeabilized HEK-293 cells. In panel *C*, $dGB2^{\Delta C2}$ overlapped with calreticulin (91.8 ± 1.2 %), but not $dGB2^{\Delta C1}$ (1.8 ± 0.4 %). In panel *E*, dGB2 and calreticulin overlapped in the bottom panel (89.9 ± 0.1 %) but not in the top panel (3.9 ± 0.5 %). **(D and F)** ELISA measurement of the amount of HA-tagged dGB1 constructs at the cell surface when co-expressed with the indicated Flag-tagged dGB2. Data represent the means ± SEM from three independent experiments, one-way ANOVA test. ns, non significance,

**** $p<0.0001$. In panel A-C, values indicate the mean ± SEM from three independent experiments. Scale bar, 10 μm. Insets: enlarged areas as indicated.

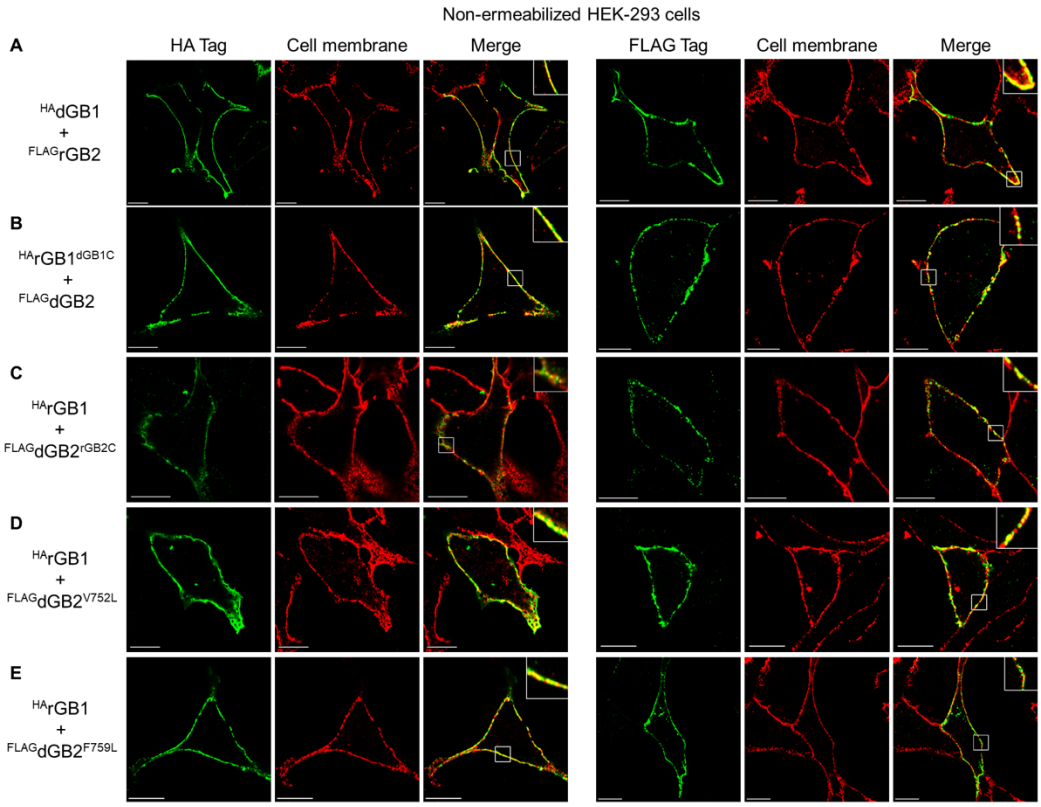

Figure S4. Various recombination of rat and drosophila $GABA_B$ receptor subunits in the cell surface. Fluorescent detection of the indicated drosophila or rat HA-tagged GB1 and FLAG-tagged GB2 constructs co-expressed, and Na,K-ATPase α_1, from permeabilized HEK-293 cells. Overlapping with Na,K-ATPase α_1 was quantified for dGB1 and rGB2 (66.4 ± 2.8 % and 77.0 ± 1.8 %, respectively) ***(A)***, $rGB1^{dGB1C}$ and dGB2 (70.1 ± 0.6 % and 70.1 ± 0.6 %) ***(B)***, rGB1 and $dGB2^{rGB2C}$ (93.1 ± 3.6 % and 90.6 ± 0.1 %) ***(C)***, rGB1 and $dGB2^{V752L}$ (75.8 ± 3.1 % and 70.9 ± 1.4 %) ***(D)*** , rGB1 and $dGB2^{F759L}$ (76.6 ± 2.5 % and 65.0 ± 1.9 %) ***(E)***. Values indicate the mean ± SEM from three independent experiments. Scale bar, 10 µm. Insets: enlarged areas as indicated.

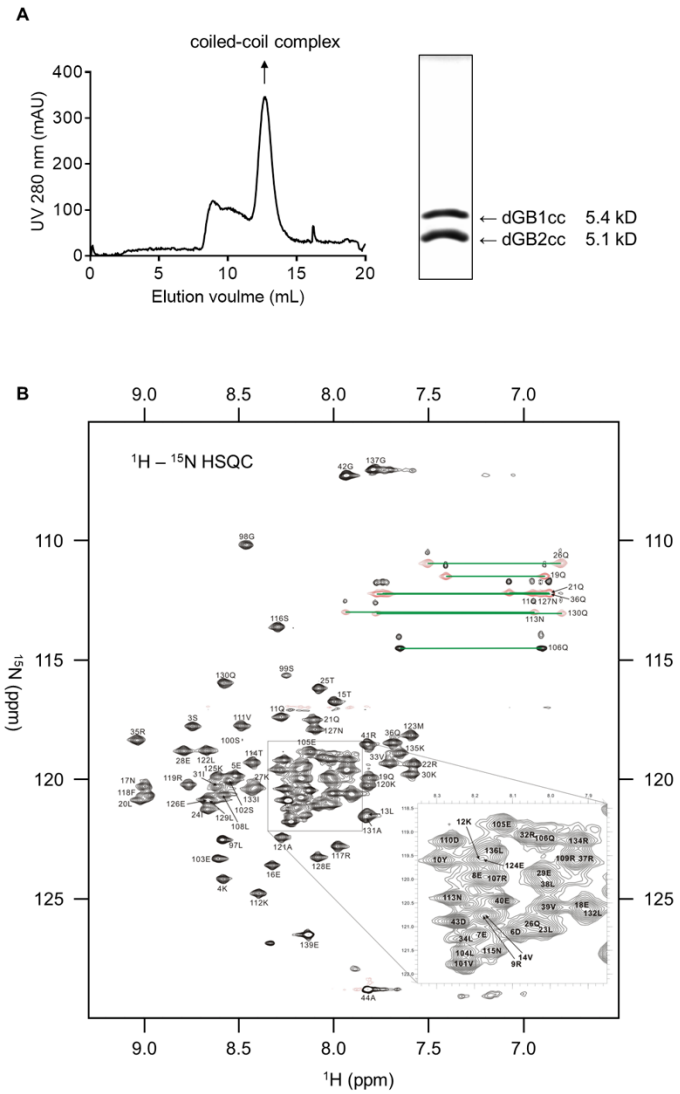

Figure S5. Purification and NMR analysis of the recombinant coiled-coil domain complex. (A) Representative size exclusion chromatography profile of the purified isotope-labeled coiled-coil domain complex. Peak tubes were pooled and identified by tricine SDS-PAGE. Arrows indicate the polypeptides dGB1cc and dGB2cc. **(B)** 2D ^{1}H-^{15}N HSQC spectrum of uniformly ^{15}N-labeled coiled-coil domain in 20 mM pH 7.0 phosphate buffer showing amide proton to nitrogen correlations for the indicated residues.

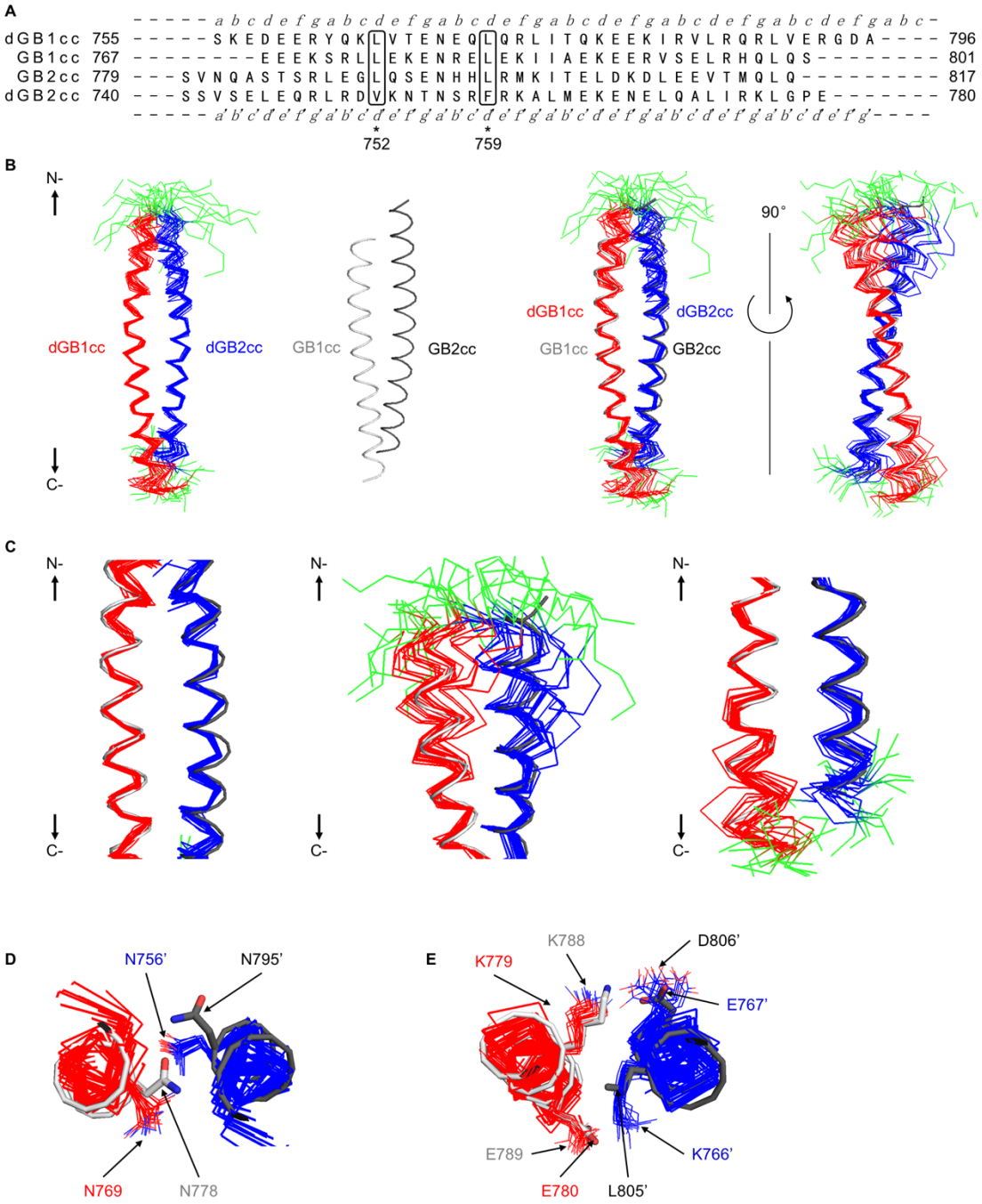

Figure S6. Comparison of the structures of the cc domain for the drosophila and mammals. (A) Protein sequence alignment of the dGB1cc and dGB2cc constructs with that of mammals, based on the crystal structure of the $GABA_B$ receptor coiled-coil domain (PDB *4PAS*) previously reported, and our present NMR solution structure. **(B)** Structural alignment of NMR solution structures of dGB1cc:dGB2cc and the mammalian GB1cc:GB2cc (PDB *4PAS*) complexes. Molecular models were

generated individually and their backbone were superimposed by Pymol. **(C)** Close up view of the central, N- and C-terminal parts of these surimposed structures. **(D)** The hydrogen bond Asn-Asn interaction between GB1 and GB2 is conserved. **(E)** Only one of the two interhelical salt bridges identified in drosophila cc domain is conserved in mammals.

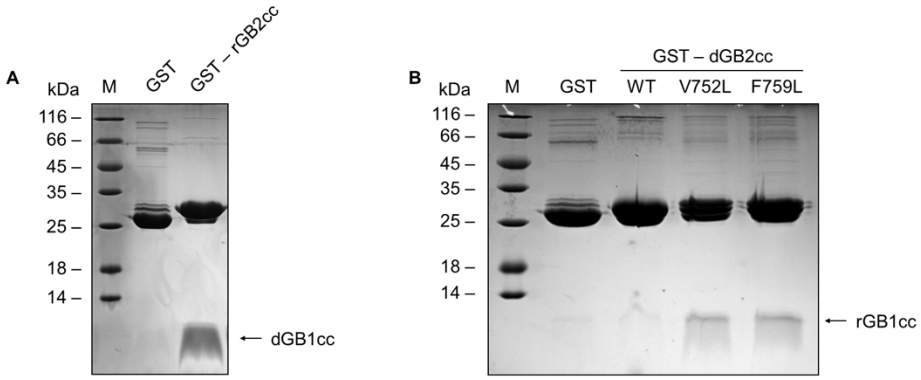

Figure S7. **Biochemical evidence of coiled-coil interaction between rat and *drosophila* GABA$_B$ receptor. (A)** Pull down of the His-tagged dGB1cc polypeptide (dGB1cc) by the recombinant GST-tagged rGB2 coiled-coil region (rGB2cc). **(B)** Pull down of the His-tagged rGB1cc polypeptide (rGB1cc) by the recombinant GST-tagged dGB2 coiled-coil region either wild-type (WT) or mutated (V752L or F759L). Unmodified GST was used as negative control.

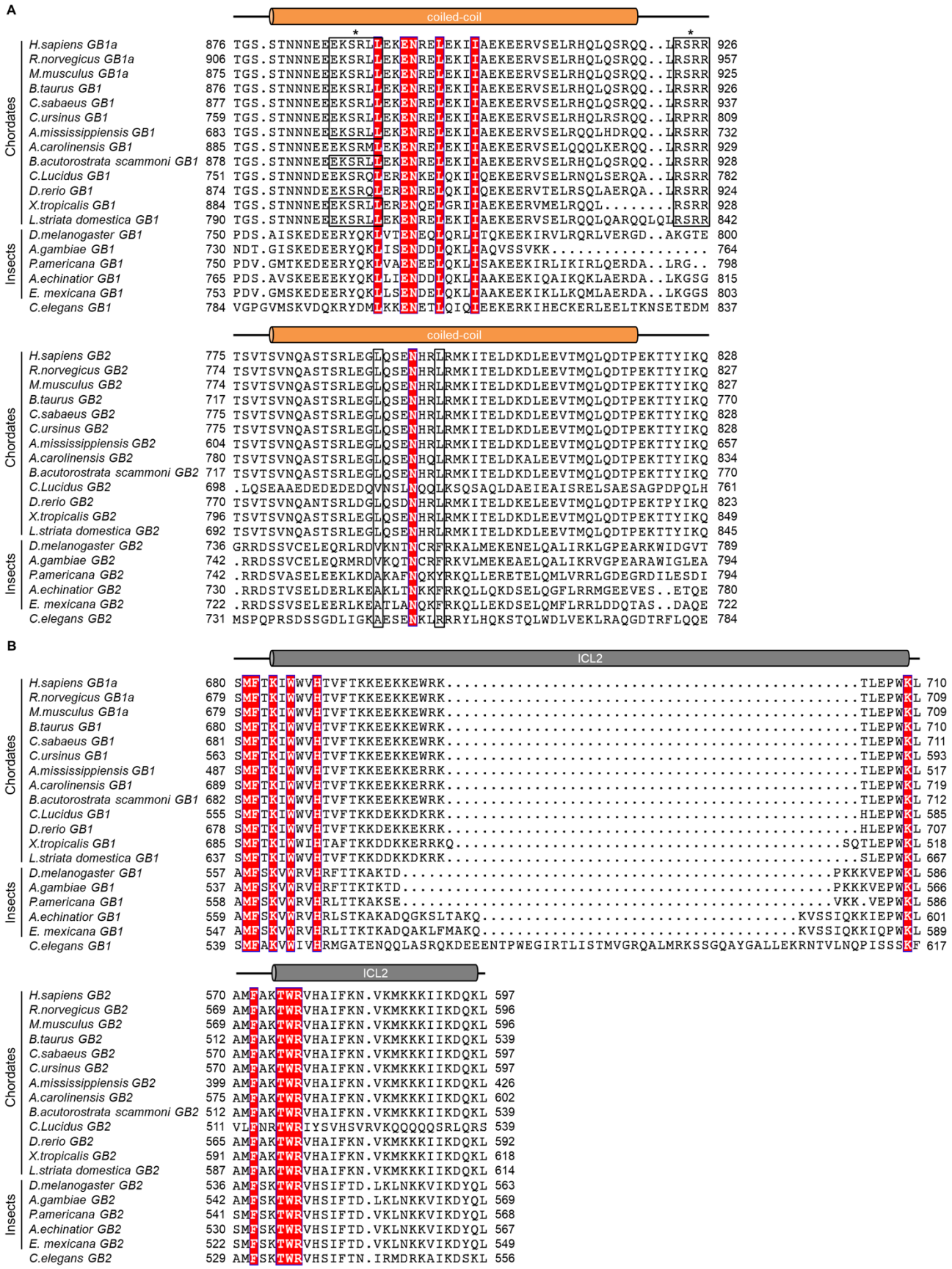
A
coiled-coil
Chordates
Insects
H.sapiens GB1a 876 TGS.STNNNEEEKSRLLEKENRELEKILAEKEERVSELRHQLQSRQQ..LRSRR 926
R.norvegicus GB1a 906 TGS.STNNNEEEKSRLLEKENRELEKILAEKEERVSELRHQLQSRQQ..LRSRR 957
M.musculus GB1a 875 TGS.STNNNEEEKSRLLEKENRELEKILAEKEERVSELRHQLQSRQQ..IRSRR 925
B.taurus GB1 876 TGS.STNNNEEEKSRLLEKENRELEKILAEKEERVSELRHQLQSRQQ..LRSRR 926
C.sabaeus GB1 877 TGS.STNNNEEEKSRLLEKENRELEKILAEKEERVSELRHQLQSRQQ..LRSRR 937
C.ursinus GB1 759 TGS.STNNNEEEKSRLLEKENRELEKILAEKEERVSELRHQLRSRQQ..LRPRR 809
A.mississippiensis GB1 683 TGS.STNNNEEEKSRLLEKENRELEKILAEKEERVSELRQQLHDRQQ..LRSRR 732
A.carolinensis GB1 885 TGS.STNNNEEEKSRMLEKENRELEKILAEKEERVSELQQQLKERQQ..LRSRR 929
B.acutorostrata scammoni GB1 878 TGS.STNNNEEEKSRLLEKENRELEKILAEKEERVSELRHQLQSRQQ..LRSRR 928
C.Lucidus GB1 751 TGS.STNNNDEEKSRQLERENKELQKILQEKEERVSELRNQLSERQA..LRSRR 782
D.rerio GB1 874 TGS.STNNNDEEKSRQLERENRELQKILQEKEERVTELRSQLAERQA..LRSRR 924
X.tropicalis GB1 884 TGS.STNNNEEEKSRLLERENQELGRILAEKEERVMELRQQL.....RSRR 928
L.striata domestica GB1 790 TGS.STNNNEEEKSRLLEKENRELEKILAEKEERVSELRQQLQARQQLQLRSRR 842
D.melanogaster GB1 750 PDS.AISKEDEERYQKLVTENEQLQRLITQKEEKIRVLRQRLVERGD..AKGTE 800
A.gambiae GB1 730 NDT.GISKEDEERYQKLISENDDLQKLIAQVSSVKK..... 764
P.americana GB1 750 PDV.GMTKEDEERYQKLVAENEELQKLISAKEEKIRLIKIRLQERDA..LRG.. 798
A.echinatior GB1 765 PDS.AVSKEEEEKYQKLLIENDDLQKLIAAKEEKIQAIKQKLAERDA..LKGSG 815
E. mexicana GB1 753 PDV.GMSKEDEERYQKLLSENDELQKLIAAKEEKIKLLKQMLAERDA..LKGGS 803
C.elegans GB1 784 VGPGVMSKVDQKRYDMLKKENETLQIQLEEKERKIHECKERLEELTKNSETEDM 837
coiled-coil
H.sapiens GB2 775 TSVTSVNQASTSRLEGLQSENHRLRMKITELDKDLEEVTMQLQDTPEKTTYIKQ 828
R.norvegicus GB2 774 TSVTSVNQASTSRLEGLQSENHRLRMKITELDKDLEEVTMQLQDTPEKTTYIKQ 827
M.musculus GB2 774 TSVTSVNQASTSRLEGLQSENHRLRMKITELDKDLEEVTMQLQDTPEKTTYIKQ 827
B.taurus GB2 717 TSVTSVNQASTSRLEGLQSENHRLRMKITELDKDLEEVTMQLQDTPEKTTYIKQ 770
C.sabaeus GB2 775 TSVTSVNQASTSRLEGLQSENHRLRMKITELDKDLEEVTMQLQDTPEKTTYIKQ 828
C.ursinus GB2 775 TSVTSVNQASTSRLEGLQSENHRLRMKITELDKDLEEVTMQLQDTPEKTTYIKQ 828
A.mississippiensis GB2 604 TSVTSVNQASTSRLEGLQSENHRLRMKITELDKDLEEVTMQLQDTPEKTTYIKQ 657
A.carolinensis GB2 780 TSVTSVNQASTSRLEGLQSENHQLRMKITELDKALEEVTMQLQDTPEKTTYIKQ 834
B.acutorostrata scammoni GB2 717 TSVTSVNQASTSRLEGLQSENHRLRMKITELDKDLEEVTMQLQDTPEKTTYIKQ 770
C.Lucidus GB2 698 .LQSEAAEDEDEDEDQVNSLNQQLKSQSAQLDAEIEAISRELSAESAGPDPQLH 761
D.rerio GB2 770 TSVTSVNQANTSRLDGLQSDNHRLRMKITELDKELEEVTMQLQDTPEKTPYIKQ 823
X.tropicalis GB2 796 TSVTSVNQASTSRLEGLQSENHRLRMKITELDKDLEEVTMQLQDTPEKTTYIKQ 849
L.striata domestica GB2 692 TSVTSVNQASTSRLEGLQSENHRLRMKITELDKDLEEVTMQLQDTPEKTTYIKQ 845
D.melanogaster GB2 736 GRRDSSVCELEQRLRDVKNINCRFRKALMEKENELQALIRKLGPEARKWIDGVT 789
A.gambiae GB2 742 .RRDSSVCELEQRMRDVKQTNCRFRKVLMEKEAELQALIKRVGPEARAWIGLEA 794
P.americana GB2 742 .RRDSVASELEEKLKDAKAFNQKYRKQLLERETELQMLVRRLGDEGRDILESDI 794
A.echinatior GB2 730 .RRDSTVSELDERLKEAKLTNKKFRKQLLQKDSELQGFLRRMGEEVES..ETQE 780
E. mexicana GB2 722 .RRDSSVSELEERLKEATLANQKFRKQLLEKDSELQMFLRRLDDQTAS..DAQE 722
C.elegans GB2 731 MSPQPRSDSSGDLIGKAESENKLRRRYLHQKSTQLWDLVEKLRAQGDTRFLQQE 784
B
ICL2
H.sapiens GB1a 680 SMFTKIWWVHTVFTKKEEKKEWRK.....TLEPWKL 710
R.norvegicus GB1a 679 SMFTKIWWVHTVFTKKEEKKEWRK.....TLEPWKL 709
M.musculus GB1a 679 SMFTKIWWVHTVFTKKEEKKEWRK.....TLEPWKL 709
B.taurus GB1 680 SMFTKIWWVHTVFTKKEEKKEWRK.....TLEPWKL 710
C.sabaeus GB1 681 SMFTKIWWVHTVFTKKEEKKEWRK.....TLEPWKL 711
C.ursinus GB1 563 SMFTKIWWVHTVFTKKEEKKEWRK.....TLEPWKL 593
A.mississippiensis GB1 487 SMFTKIWWVHTVFTKKEEKKERRK.....TLEPWKL 517
A.carolinensis GB1 689 SMFTKIWWVHTVFTKKEEKKERRK.....TLEPWKL 719
B.acutorostrata scammoni GB1 682 SMFTKIWWVHTVFTKKEEKKEWRK.....TLEPWKL 712
C.Lucidus GB1 555 SMFTKIWWVHTVFTKKDEKKDKRK.....HLEPWKL 585
D.rerio GB1 678 SMFTKIWWVHTVFTKKDEKKEKRK.....HLEPWKL 707
X.tropicalis GB1 685 SMFTKIWWIHTAFTKKDDKKERRKQ.....SQTLEPWKL 518
L.striata domestica GB1 637 SMFTKIWWVHTVFTKKDDKKDKRK.....SLEPWKL 667
D.melanogaster GB1 557 AMFSKVWRVHRFTTKAKTD.....PKKKVEPWKL 586
A.gambiae GB1 537 AMFSKVWRVHRFTTKTKTD.....PKKKVEPWKL 566
P.americana GB1 558 AMFSKVWRVHRLTTKAKSE.....VKK.VEPWKL 586
A.echinatior GB1 559 AMFSKVWRVHRLSTKAKADQGKSLTAKQ.....KVSSIQKKIEPWKL 601
E. mexicana GB1 547 AMFSKVWRVHRLTTKTKADQAKLFMAKQ.....KVSSIQKKIQPWKL 589
C.elegans GB1 539 SMFAKVWIVHRMGATENQQLASRQKDEEENTPWEGIRTLISTMVGRQALMRKSSGQAYGALLEKRNTVLNQPISSSKF 617
ICL2
H.sapiens GB2 570 AMFAKTWRVHAIFKN.VKMKKKIIKDQKL 597
R.norvegicus GB2 569 AMFAKTWRVHAIFKN.VKMKKKIIKDQKL 596
M.musculus GB2 569 AMFAKTWRVHAIFKN.VKMKKKIIKDQKL 596
B.taurus GB2 512 AMFAKTWRVHAIFKN.VKMKKKIIKDQKL 539
C.sabaeus GB2 570 AMFAKTWRVHAIFKN.VKMKKKIIKDQKL 597
C.ursinus GB2 570 AMFAKTWRVHAIFKN.VKMKKKIIKDQKL 597
A.mississippiensis GB2 399 AMFAKTWRVHAIFKN.VKMKKKIIKDQKL 426
A.carolinensis GB2 575 AMFAKTWRVHAIFKN.VKMKKKIIKDQKL 602
B.acutorostrata scammoni GB2 512 AMFAKTWRVHAIFKN.VKMKKKIIKDQKL 539
C.Lucidus GB2 511 VLFNRTWRIYSVHSVRVKQQQQQSRLQRS 539
D.rerio GB2 565 AMFAKTWRVHAIFKN.VKMKKKIIKDQKL 592
X.tropicalis GB2 591 AMFAKTWRVHAIFKN.VKMKKKIIKDQKL 618
L.striata domestica GB2 587 AMFAKTWRVHAIFKN.VKMKKKIIKDQKL 614
D.melanogaster GB2 536 AMFSKTWRVHSIFTD.LKLNKKVIKDYQL 563
A.gambiae GB2 542 AMFSKTWRVHSIFTD.LKLNKKVIKDYQL 569
P.americana GB2 541 SMFSKTWRVHSIFTD.VKLNKKVIKDYQL 568
A.echinatior GB2 530 SMFSKTWRVHSIFTD.VKLNKKVIKDYQL 567
E. mexicana GB2 522 SMFSKTWRVHSIFTD.VKLNKKVIKDYQL 549
C.elegans GB2 529 AMFSKTWRVHSIFTN.IRMDRKAIKDSKL 556

Figure S8. Amino acid sequences alignment of $GABA_B$ receptor for the cc domain (A) and ICL2 (B). Sequences are from National Center for Biotechnology Information Protein database (http://www.ncbi.nlm.nih.gov). The alignment was generated with ClustalW and was displayed with ESPript 3. Alignment is according to full-length $GABA_B$ receptor sequence. The most conserved residues were highlighted in red background.. The conserved di-leucine (EKSRLL) and RxRR motifs (black outline) in chordates were highlighted (asterisk). The positions equivalent to the residues 752 and 759 of dGB2 are indicated.

The species abbreviations are: H. sapiens, Homo sapiens; R. norvegicus, Rattus norvegicus; M. musculus, Mus musculus; B. taurus, Bos taurus; C. sabaeus, Chlorocebus sabaeus; C. ursinus, Callorhinus ursinus; A. mississippiensis, Alligator mississippiensis; A. carolinensis, Anolis carolinensis; B. acutorostrata scammoni, Balaenoptera acutorostrata scammoni; C. lucidus, Collichthys lucidus; D. rerio, Danio rerio; X. tropicalis, Xenopus tropicalis; L. striata domestica, Lonchura striata domestica; D. melanogaster, Drosophila melanogaster; A. gambiae, Anopheles gambiae; P. americana, Periplaneta americana; A. echinatior, Acromyrmex echinatior; E. mexicana, Eufriesea mexicana; C. elegans, Caenorhabditis elegans.

Table S1. Sequence identity and divergence of human, rat and *drosophila* $GABA_B$ receptor subunits.

Percent identity

Divergence

	hGB1a	hGB1b	hGB2	rGB1e	rGB1c	rGB2	dGB1	dGB2
hGB1a	***	95.9	32.1	98.8	95.3	32	47	30.3
hGB1b	4.3	***	32.9	95.1	98.5	32.9	47	30.4
hGB2	147.8	143.2	***	32.1	32.9	97.8	32.2	40
rGB1e	1.3	5	147.8	***	96.3	32	46.8	30.4
rGB1c	4.9	1.6	143.2	3.8	***	32.9	46.8	30.4
rGB2	148.2	143	2.3	148.2	143	***	32.2	39.7
dGB1	88.3	88.3	147.2	88.7	88.7	147.2	***	30.5
dGB2	158.2	157.5	111.5	157.5	157.5	112.7	157.1	***

Table S2. Structural statistics for the family of 20 structures of dGB1cc:dGB2cc in aqueous solution.

Total number of distance restraints	1254
Intra residue (|i-j|=0)	595
Sequential (|i-j|=1)	267
Mediate range (1<|i-j|<5)	197
Long range (|i-j|>=5)	80
ambiguous restraints	52
Hydrogen bond	63
Dihedral angle restraints	
Φ	73
Ψ	72
Mean rmsd from idealized covalent geometry	
bond (Å)	3.291e-3 ± 1.262e-4
angle (°)	4.887e-1 ± 1.923e-2
Improper (°)	1.204 ± 6.632e-2
Mean rmsd from the experimental restraints	
dihedral angle (°)	9.778e-2 ± 8.440e-2
distance (Å)	3.473e-2 ± 4.870e-3
Ramachandran plot*	
% residues in the most favorable regions	99.5%
additional allowed regions	0.5%
generously allowed regions	0%
Atomic rmsd	
backbone	0.63 ± 0.22**
heavy atoms	1.63 ± 0.18**
Notes	
*results from psvs version 1.5 (psvs-1_5-dev.nesg.org) **selected residues: chain A 6-23 and chain B 104-122	

Table S3. GABA potency for the indicated constructs co-expressed together in HEK-293 cells and measured by intracellular calcium release assays. Data represent the means ± SEM of (n) independent experiments.

Heterodimer	pEC_{50}
rGB1 – rGB2	7.850 ± 0.016 (6)
dGB1 – dGB2	5.963 ± 0.007(12)
dGB1 – $dGB2^{\Delta C1}$	5.916 ± 0.015 (3)
$dGB1^{\Delta C1}$ – dGB2	5.935 ± 0.014 (3)
dGB1 – rGB2	5.893 ± 0.005 (3)
$rGB1^{dGB1C}$ – dGB2	5.900 ± 0.003 (3)
rGB1 – $dGB2^{rGB2C}$	5.891 ± 0.003 (3)
rGB1 – $dGB2^{V752L}$	5.314 ± 0.005 (3)
rGB1 – $dGB2^{F759L}$	5.278 ± 0.007 (3)